Nordisk kernesikkerhedsforskning
Norrænar kjarnöryggisrannsóknir
Pohjoismainen ydinturvallisuustutkimus
Nordisk kjernesikkerhetsforskning
Nordisk kärnsäkerhetsforskning
Nordic nuclear safety research

NKS-83
ISBN 87-7893-140-1

Recriticality Calculation with GENFLO Code for the BWR Core After Steam Explosion in the Lower Head

Jaakko Miettinen
VTT Processes, Finland

December 2002

Abstract

Recriticality of the partially degraded BWR core has been studied by assuming a severe accident phase during which the fuel rods are still intact but the control rods have experienced extensive damage. Previous NKS and EU projects have studied the same case assuming reflooding by the ECCS system In the present study it was assumed that coolant enters the core due to melt-coolant interaction in the lower plenum. In the first case specified the relocation and fragmentation of the molten control rod metal causes the level swell in the core but no steam explosion. In the second case a steam explosion in the lower head was assumed.

In the first case a prompt recriticality peak can occur, but after the peak no semistable power generation remains. In the second case the consequence of the slug entrance into the core is so violent that the fuel disintegration and melting during the first power peak may occur. After the large power peak water is rapidly pushed back from the core and no semistable power generation maintains. The fuel disintegration studies have been based on a coarse assumption that the acceptable local energy addition into the fresh fuel may be 170 cal/g, but with increasing burn-up it can be as low as 60-70 cal/g. In the level swell variations the maximum energy addition was between these limits, but in most of the steam explosion variations much above these limits. Additional variation of the assumptions related to the neutronics demonstrated that for the converged analysis result some interactions would be useful with respect to the boundary conditions and neutronic options.

Key words

Severe accidents, re-criticality, melt-coolant interaction

NKS-83
ISBN 87-7893-140-1

Pitney Bowes Management Services Denmark A/S, 2003

The report can be obtained from
NKS Secretariat
P.O. Box 30
DK – 4000 Roskilde, Denmark

Phone +45 4677 4045
Fax +45 4677 4046
www.nks.org
e-mail nks@catscience.dk

RECRITICALITY CALCULATION WITH GENFLO CODE FOR THE BWR CORE AFTER STEAM EXPLOSION IN THE LOWER HEAD

Jaakko Miettinen

VTT Processes

PREFACE

Prof. Raj Sehgal from KTH Stockholm evaluated the conditions for the steam explosion. Mr. Risto Sairanen defined the preliminary conditions after the control rod melting. The study was a joint effort done by VTT and KTH, financed by NKS, STUK and SKI.

CONTENTS

1. INTRODUCTION

Recriticality due to entry of a two-phase mixture or a slug of water into the BWR core devoid of control rods has been investigated in Finland in several previous studies.

Anttila (1990) evaluated that the coolant reflooding the core with void fraction content of 0% has to reach at least 0.4 m to pose a threat of prompt-criticality and with void fraction of 60% at least 1.0 meter for the same effect.

Okkonen, Hyvärinen and Haule (1993) evaluated with RELAP5, how much boiling due to melt fragmentation in the lower plenum is needed for the core reflooding, and recriticality. The melt mass was large, i.e., 4-8 tonnes in a well fragmented state (1 mm particle size diameter partially, and 10 mm for the rest). Varying the particle sizes yielded 200 to 2500 MW between 12 to 0.5 seconds.

Recriticality for a BWR core devoid of control rods has been studied by Hoejerup et al. (1997) and continued by Frid at al. (1999) in the SARA project, performed in the European Union 4th Framework program. The studies focused on core reflood by ECCS during the early part of a postulated severe accident when the control rods have melted but the fuel rod bundles are intact. Three different computer programs - RECRIT, APROS and SIMULATE-3K - were applied as analysis tools. The prompt recriticality peak was achieved by all reflooding rates (160 – 1350 kg/s) after the first recriticality and its total energy was the function of the reflooding rate. The prompt criticality was terminated with the Doppler feed back, however, substantial energy was deposited in the fuel rods.

The objective of the current work was to investigate if melt relocating to the lower plenum can cause a steam explosion, and if this steam explosion can cause core recriticality. The main focus in the FCI research done past has been the steam explosion, which could directly fail the containment. The probability for this kind of failure has been found negligible small, but at the same time the research work has produced a lot of interesting information, which can be applied for evaluation of the milder consequences.

The initial accident scenario for the BWR plant may be described as follows: The full blackout means the reduction in the coolant balance of the vessel. For initiating the LPCI the ADS relief valve is opened for depressurization of the reactor system. It was assumed that LPCI fails to start. This scenario leads to the core heatup, and boiling of the coolant inventory until its level is below the core plate.

It is postulated that the BWR core is degraded so far that the control rods have already melted and molten control rod material is available on top of the core plate.. The molten eutectic mixture of B_4C and steel is filling the space between the fuel canisters. By postulating a failure of the core support plate the molten metal pours into the water pool in the lower head and FCI conditions are encountered. The melt-water interaction in the lower head can occur in energetic (steam explosion) and non-explosive way. The latter means strong evaporation in the lower plenum, which may push a slug of the two-phase mixture into the downcomer and core regions. In the energetic FCI the single phase liquid may enter the core.

Two possibilities exist, how the molten material may fall into the lower plenum. The canister wall may be eroded by the molten metal and it flows down through the fuel inlet passage. Another possibility is that the largely molten control rod is relocated from its position, allowing the molten metal to discharge down.

The analysis was shared between VTT and KTH. The task of KTH was evaluation of the steam explosion process itself. The task of VTT was analysis of the recriticality phase of the accident, based on the flow boundary conditions defined by KTH. This report summarises the GENFLO analyses for the recriticality, based on the reflooding due to the energetic or non-energetic fuel-coolant interaction defined by KTH (Sehgal & Dinh 2002).

2. RECRITICALITY FEATURES IN THE GENFLO APPLICATIONS

2.1. GENFLO GENERAL FEATURES

The RECRIT code was the origin of the GENFLO code used for the analyses. RECRIT combined the two-dimensional neutronics solution developed at Risø National Laboratory and BWR focused thermohydraulic developed at VTT Energy. The combined model can simulate the BWR recriticality scenario from the beginning of the postulated blackout incident to the reflooding process of the core and recriticality caused by the reflooding water entering the core.

The first version of RECRIT, written at Risø National Laboratory, had simple but sound models for neutronics but carried some significant modelling undershootings in thermal hydraulic parts (Hoejerup, 1997b). These deficiencies were remedied with combining thermal hydraulic models developed at VTT Energy and the 2D neutronics models of the original RECRIT code..

The present analyses were carried out with the renewed version of the RECRIT code, called GENFLO. The GENFO code combines the thermohydraulic analysis tool for three purposes:

1) In fuel rod transient analysis application the same thermohydraulic solution is used as a subchannel model of the FRAPTRAN code,

2) In APROS-SA (severe accident module in APROS) application the same thermohydraulic content is used for simulating the degraded core thermohydraulics, with relocation and melt pool formation.

3) Original RECRIT application for the BWR recriticality.

The modelling of the thermohydraulics and neutronics related to the recriticality analyses is described in the separate report (Miettinen 1999) and the GENFLO thermohydraulics without neutronics part in (Hämäläinen & Miettinen 2002) The results of the GENFLO thermohydraulic validation are described in (Miettinen 1999).

2.2. THE RECRITICALITY CONSIDERED IN GENFLO

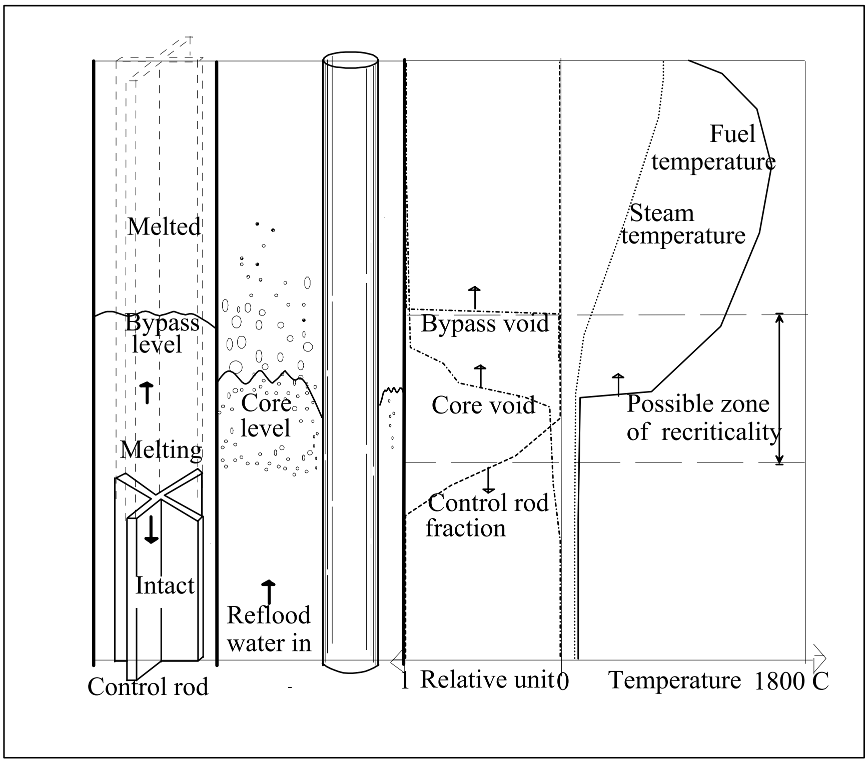

Figure 1. *Illustration of conditions for the local recriticality.*

The key phenomena around the recriticality of the degraded core during the bottom re-flooding are illustrated in Fig. 1. During reflooding a quenching front moves through the core. The region below the quench front contains bubbles in single phase liquid (void fraction < 0.3, cladding saturated) while the region above it has droplets in gas (void fraction > 0.8, cladding superheated). This distribution profile moves upwards and when it reaches the core location devoid of control rods, the recriticality with power excursion is possible.

GENFLO simulates the entire BWR vessel geometry, as presented in Fig. 2. The real plant sections are described for the downcomer, lower plenum, core, bypass, upper ple-num, steam separator and steam dome. The input data has been minimized by hard-wiring the process model into lumped sections. The calculation level nodalization is generated by the preprocessor from the lumped data. The sections outside the core are one-dimensional components. The injections are described for HPCIS as a time depend-ent injection and LPCIS as a pressure dependent injection. The steam release is de-scribed for the relief, safety and ADS valves.

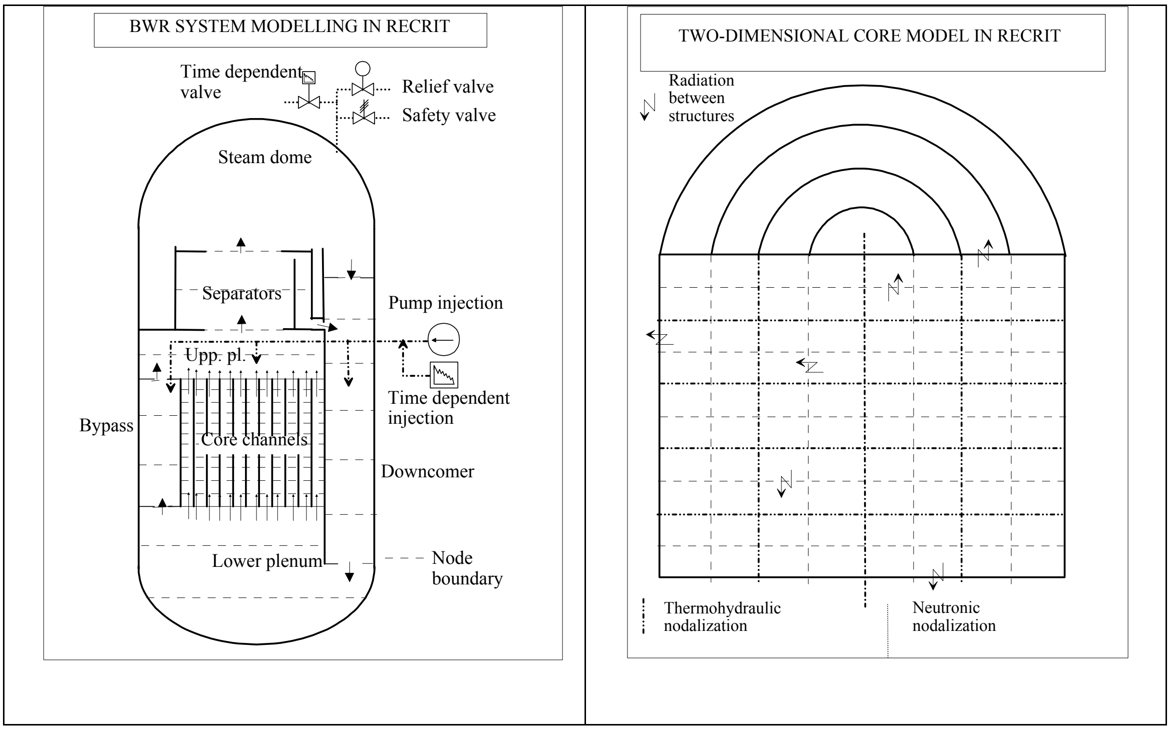

Figure 2. Plant and core description in RECRIT

The core is described by a two-dimensional model, cylindrical geometry with 10-100 axial nodes and 3-20 radial rings. The neutronic nodes are related to fuel rod heat structures. The radial rings have an equal thickness. The fuel rod structure describes the cladding, gas gap and pellet. The core power is attached to the pellet, the oxidation to the cladding. The approach selected for the coupling of the neutronics and reflooding thermohydraulics has been depicted in Fig. 3.

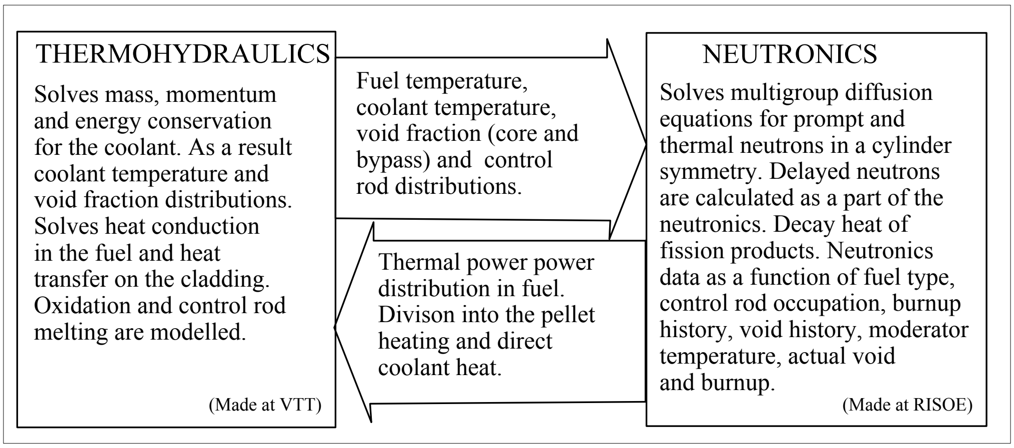

***Figure 3.** Transfer of information between the neutronic and thermohydraulic module.*

2.3. SOLUTION OF THE NEUTRONICS

The neutron flux distributions and reactivities are calculated with a standard diffusion theory, multigroup, difference approximation code (Hoejerup, 1997a). The calculation includes the interpolation for cross sections, the flux, the number of spontaneous fission neutrons emitted by U238 and the heat dissipation from the fission products in the fuel.

The infinite multiplication factor, k_{inf}, is defined for the two-group presentation by

$$k_{inf} = \frac{\nu_1\, \Sigma_1^f * \Sigma_{22} + \nu_2\, \Sigma_2^f * \Sigma_{12}}{\Sigma_{11} * \Sigma_{22}} \tag{1}$$

The concentrations, C_i, of the delayed neutron precursors is calculated as:

$$C_i^{(n)} = C_i^{(n-1)}\, e^{-\lambda_i \Delta t^{(n)}} + \beta_i \sum_g \left(\nu\Sigma^f\right)_g \Phi_g^{(n-1)} \left(1 - e^{-\lambda_i \Delta t^{(n)}}\right) / \lambda_I \tag{2}$$

where β_i and λ_i are the yield and the decay constant of the i' th group of delayed neutron precursors. The neutrons emitted by the delayed neutron precursors are added to the neutrons from the spontaneous fissions in U^{238}. The neutronic solution is originally a steady-state, standard diffusion theory, multigroup, difference approximation. For the use in power excursion analyses the time derivative has been added into the neutron flux

$$D_g \nabla^2 \Phi_g - \Sigma_{gg} \Phi_g + \sum_{g' \neq g} \Sigma_{g'g} \Phi_{g'} + \lambda\, \xi_g \sum_{g'} (\nu\ \Sigma^f)_{g'} \Phi_{g'} + Q_g = \frac{1}{v_g} \frac{\partial \Phi_g}{\partial t} \tag{3}$$

where the time derivative is approximated by

$$\frac{1}{v_g} \frac{\partial \Phi_g}{\partial t} = \frac{1}{v_g} \frac{\Phi_g^{(n)} - \Phi_g^{(n-1)}}{\Delta t^{(n)}} \tag{4}$$

where $\Phi_g^{(n)} = \Phi_g$ is interpreted as the flux to be determined,
$\Phi_g^{(n-1)}$ is the flux from the previous time step, and
$\Delta t^{(n)}$ is the length of the time step.

Equation (3) with the discretization of the right hand side may be solved with respect to the neutron flux. The standard diffusion parameters, D, Σ, v_g are given as functions of the control rod concentration, coolant and fuel conditions. An important feature is to select a proper time steps. The eigenvalue, $(1/k_{eff})$, is the key parameter for the proper time step. In the rapid power excursion the timestep is typically 0.1 ms.

The diffusion parameters of the individual neutronic nodes are interpolated in 7-dimensional tables as functions of

1. fuel type,
2. control rod occupancy,
3. void fraction history during the earlier operation,

4. fuel temperature,
5. moderator temperature,
6. actual void and
7. burnup.

The precalculated tables are defined for 2 group parameters :

D_1 , D_2	: diffusion coefficients
$\Sigma_{1,1}$, $\Sigma_{2,1}$, $\Sigma_{1,2}$, $\Sigma_{2,2}$	: diffusion matrix
$\nu_1\Sigma_1^f$, $\nu_2\Sigma_2^f$	: reproduction cross sections
Σ_1^f, Σ_2^f	: fission cross sections
v_1, v_2	: neutron velocities
$\beta_{i,\ i=1,6}$	: yield of delayed neutrons
$\lambda_{i,\ i=1,6}$	: decay of delayed neutrons.

The decay heat is calculated with a simplified exponential power formula.

2.4. THERMOHYDRAULIC EQUATIONS

The basic field equations comprise two mass equations, one mixture momentum equation and two energy equations. The basic variables in the solution are

Pressure, p (Pa)
Void fraction, α (-)
Mixture velocity, u_m, (m/s)
Gas enthalpy, h_g, (J/kg)
Liquid enthalpy, h_l, (J/kg)
Concentration of noncondensables, C_N (relative 0 - 1).

The phase separation is solved by the drift flux model. The quenching front is described with the model described in (Miettinen & Höjerup 1999a and Hämäläinen & Miettinen 2002). It makes possible sharp void fraction gradients, which promote the core reactivity through the better moderation. The movement of the quenching front is controlled by conduction in the cladding. The heat transfer below the quenching front combines the forced convection for boiling. In addition to the quenching front heat transfer the post-dryout heat transfer required an own consideration. Based on visual observations from rewetting experiment, a concept was selected, where the flow above the quenching contains only droplet dispersed flow. This post dryout heat transfer contains the film boiling, transition boiling, vapour heating, interphasial heat transfer and radiation heat transfer. The cladding oxidation is described with the Urbanic / Heidrick correlation. The thermohydraulic solution is described in detail in (Hämäläinen & Miettinen 2002).

2.5. GENFLO VALIDATION PROGRAM

The origin of GENFLO, the RECRIT code has been validated against several reflooding experiments (Miettinen, 1999). Reflooding experiments in ERSEC7, FLECHT, GÖTA, ACHILLES and REWET-II facilities were selected for validation of the reflooding capabilities under these conditions. In addition, validation against recent high temperature QUENCH tests at FzK in Germany has been performed including the full local oxidation of the cladding. The experiments used in the validation are summarized in Table 1

Table 1. *Reflooding experiments for validating RECRIT thermohydraulics.*

Facility	Length (m)	T_{max} (^{o}C)	Pressure (bar)	Inflow velocity (m/s)
ERSEC -7, F (2 tests)	1 rod 3.3 m	870	1, 3	0.055
ACHILLES, UK (1 test)	69 rods 3.6 m	1050	3	Gravity feed
REWET-II, FIN, (2 tests)	19 rods 2.4 m	910	1, 3	0.02 - 0.10
GÖTA, S (14 tests)	64 rods 3.6 m	950	1, 3,7	0.008- 0.024
FLECHT,USA, (4 tests)	49 rods 3.6 m	790	1, 4, 6.7, 20	0.076
QUENCH, D, (2 tests)	21 rods 1.0 m	2100	2	0.015

The ERSEC experiment included rather large power generation and it demonstrated the flexibility of RECRIT to model different geometries. The ACHILLES experiment shows that the oscillations predicted by RECRIT are realistic although the rewetting by the gravity feed reflooding was predicted too early. The results from the GOETA were overall rather good indicating, that RECRIT models very well the reflooding conditions in the BWR fuel bundle. The result for the FLECHT were also rather good and their best value was the large pressure range. The REWET-II validation proved that RECRIT is flexible also for validating PWR experimental data. The analysis of the QUENCH experiments proved excellent calculation capability at high temperatures.

Operation of the ECCS in Swedish BWRs has been studied in GÖTA experiments. The reference plant for the experiments was the FORSMARK-1 plant, with internal circulation pumps. The schematic presentation of the experimental facility is shown in Fig. 4. The agreement in predicting the cladding temperature is demonstrated, as well. For a good agreement the water levels between different sections and quenching front location have to be properly demonstrated. A full set of comparisons is given in the RECRIT validation document (Miettinen 1999).

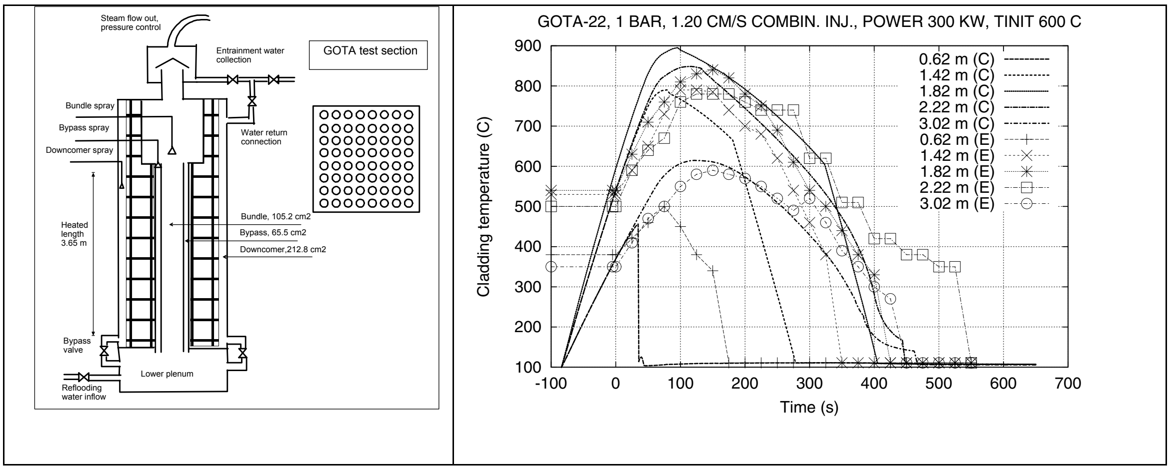

Figure 4. *GOETA facility and one comparison results for the bundle temperatures.*

3. OLKILUOTO PLANT DESCRIPTION FOR THE RECRITICALITY ANALYSES

3.1. MELCOR CALCULATIONS FOR THE CORE HEATUP

A set of MELCOR 1.8.4 Code calculations were performed. The scenario is a BWR station blackout successful depressurization, but failed ECCS start

It is assumed that the relocation of the molten control rod material into lower plenum occurs at 4700 s, when all fuel is still in initial geometry, but as much as possible control rod material is melted and removed from the core area. This assumption does not maximise the steam explosion but tries to maximise the recriticality event. The results of the MELCOR calculation for the water level history and fuel temperature behaviour has been depicted into Fig. 5.

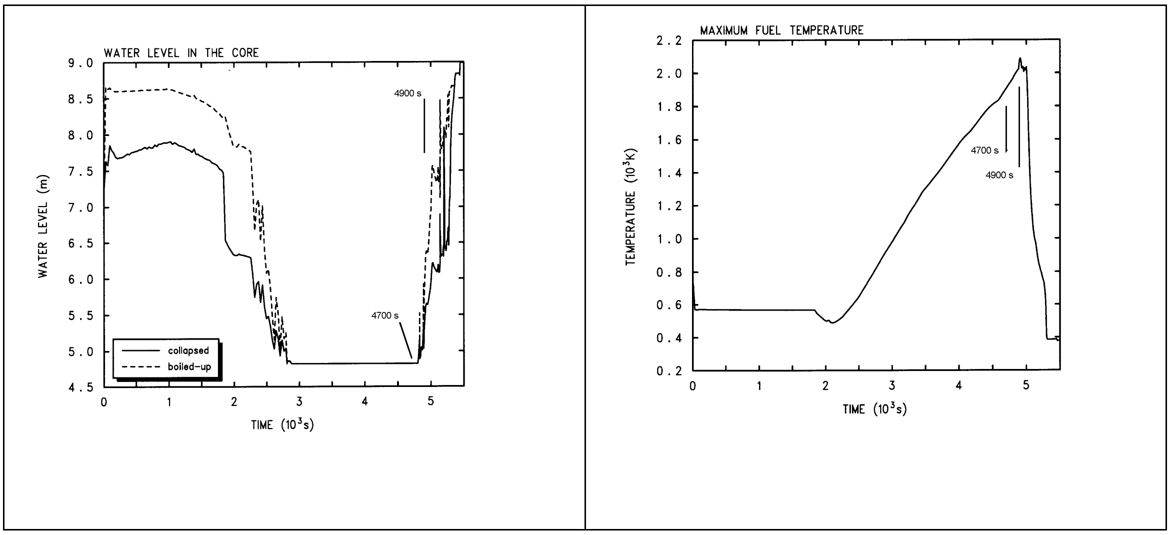

Figure 5. *Water level and fuel temperature behaviour from the MELCOR calculation.*

The initial conditions are documented in (Sairanen 2001). At 4700 s water level is below core, and 13 tons of steel and 1.1 tons of B_4C are in molten state and available for relocation. Distribution of the control rod material and the temperatures of the control rod materials are depicted. In Fig. 6

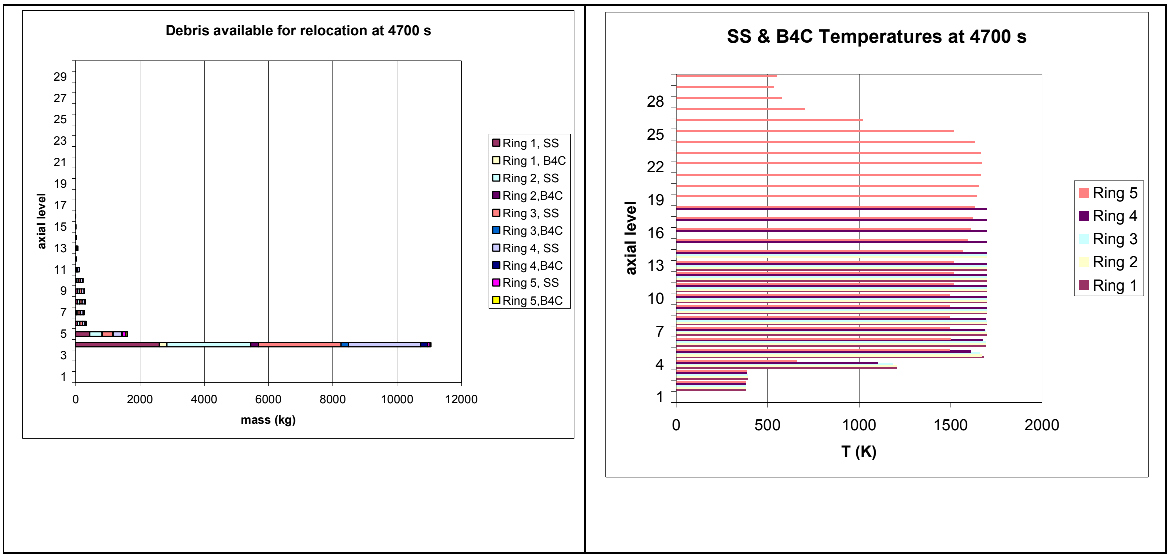

Figure 6. *Distribution of the relocated control rod material and the temperature distribution calculated by MELCOR.*

The result in Fig. 6 shows that almost all B_4C has relocated on top the core support plate in all radial rings. Control rod materials in upper elevations have temperatures above 1500 K, which indicates superheating. Most of the material is relocated to the level 4 and there the temperature is only 1000 K, below the melting point. The lower support plate may have a cooling effect.

13 tons of steel fills 1.85 m^3 and 1.1 tons B_4C fills 0.31 m^3 from the bypass area, which has a flow area of 2.1 m^2 around the fuel elements but in total with reflector sections has the flow area of 4.1 m^2. Probably the melt is not reaching the reflector area. Thus the control rod melt can create around 1 m high molten metal pool into the bypass channel.

3.2. OLKILUOTO PLANT REACTOR PHYSICAL PARAMETERS

Table 2. *Main plant data.*

Parameter	Value	Parameter	Value
Nominal core power, MWth	2500	Operation pressure, bar	70.
Number of fuel assemblies	500	Bundle inlet pressure loss, bar	0.42 – 0.56
Number of control rods	121	Bundle fuel pressure loss, bar	0.71 – 0.79
Number of circulation pumps	6	Core heat transfer area, m^2	4532.
Circulation pump flow, kg/s	7160-8200	Circulation pump flow, Atrium	7100–8300
Bundle flow, kg/s	5900-6770	Bypass flow fract., Atrium %	13.5
Core bypass flow, kg/s	1260-1430	Atrium fuel array	10x10
Bypass flow fraction, %	13.5 – 17.5	Atrium rods in assembly	91
Core average void, %	41.8 – 44.3	Svea-64 fuel array	8 x 8
Core exit void, %	70.1 – 70.3	Svea-64 rods in assembly	64
Core exit quality, -	13.2 – 15.3	Svea-96 fuel array	10x10
		Svea-96 rods in assembly	96

The main plant parameters are listed in Table 2. The important core specific data is listed in Table 3.

Table 3. *Main dimensions needed for the thermohydraulic and reactor physical input.*

Parameter	Value	Parameter	Value
O.D of a Atr. fuel rod, mm	10.03	GB CRGT area, m^2	7.75
I.D, of Atr. cladding, mm	8.84	GB CRGT length, m	3.66
Atr. clad thickness, mm	0.605	GB Lower plenum area	4.2
O.D. of Atr. fuel pellet, mm	8.67	GB Core inlet area, m^2	0.991
Effective fuel length, m	3.680	GB CRGT inlet area, m^2	0.0770
Total fuel length, m	3.977	GB downcomer area, m^2	9.31
Array of Atrium fuel	10 x 10	GB upper plenum area, m^2	14.11
Rods in Atrium assembly	91	GB steam dome area, m^2	19.1
Water space occupying	3 x 3	GB core area, m^2	5.37
Fuel flow area, m^2	0.010082	GB bypass area, m^2	4.1
Flow inlet area, m^2	0.007850	GB CRGT volume, m^3	28.5
Bypass water area per ass, m^2	0.004238	GB lower plen volume, m^3	26.7
Gap between assemblies, m	0.0142	GB downcomer volume, m^3	~85
Rod pitch, mm	12.7	Channel weight, kg	27
Number of spacers	24	Channel material	Zr-4
Inner width of fuel box, m	0.134	Atr. uranium weight, kg	177
Wall thickness of the box, m	0.0025	Atr. assembly weight, kg	292
Outer width of fuel box, m	0.139	Max. fuel burnup, MWd/kgU	40
		Max. rod burnup, MWd/kgU	51

The OlkiluotoBWR has a 2500 MW_{th}. core. Two types of fuel were assumed: Assembly type 1 includes 91 fuelled pins, among them 10 Gd rods. Assembly type 2 includes 8 additional water rods, 83 fuelled pins, and among fuel rods 9 Gd rods.

Input data to CASMO were calculated (Anttila, 1998). New CASMO-4 and TABLES-3 runs were performed for the parameter range valid for recriticality studies. The essential assumption in the data set was that the void fraction on the bypass side is equal to that on the assembly side. Note that in the normal core power condition the bypass has single phase liquid. During reflooding situation the bypass level may be higher than in the fuel channel, or if the flow route into the bypass channel is blocked, the level may be below the channel level.

The reactor physical characteristics can be studied by the multiplication factor k_{inf} which cumulates spatially the effect of different contributors to the reactivity, except the effect of the leakage. The final recriticality, interpreted through the effective multiplication factor k_{eff}, includes in addition to k_{inf} the neutron leakage. The reactor is critical by $k_{eff} = 1.000$ and prompt critical by $k_{eff} = 1 + \beta \cong 1.006$. If no leakage exists, i.e. the reactor size is infinite, $k_{eff} = k_{inf}$. Trends as a function of the void fraction, control rod concentration and fuel temperature are depicted in Fig. 7.

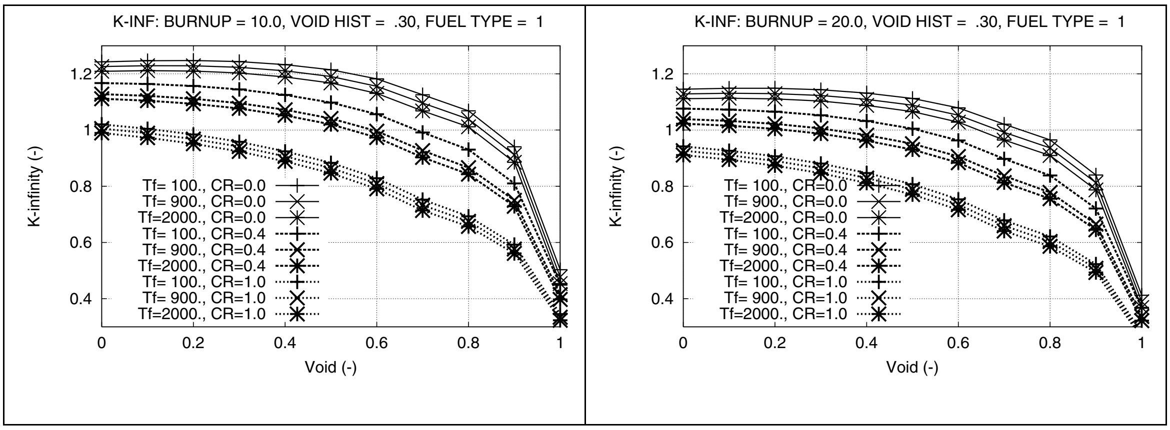

Figure 7. Infinite multiplication factor calculated from the CASMO data for 10 and 20 MWd/tU fuel, assuming fuel type 1 and void history 0.30.

The parameter trends in Fig. 7 can be used to indicate, where the reactor may become recritical. Let us use a simple criteria that the recriticality is possible, when $k_{inf} > 1.0$. It is possible if the control rods are lost and the void fraction is below 0.8. Thus the spray cooling is not sufficient for the criticality. Doppler feedback due to the fuel temperature cannot always alone compensate the excess reactivity. If reflooding water is entering the core without control rods and the void fraction drops below 0.6 ... 0.8, the local criticality is possible.

The void fraction is the strongest contributor. In the BWR core the bypass channel moderates similarly as the fuel channel. The reactor may become recritical with no water in the fuel channel, only in the bypass channel. Thus the reliable simulation of reactivity and neutron power requires reliable calculation for the void fraction, fuel temperature and control rod configuration.

In the two-dimensional approach the core is divided into axial (25) nodes and cylindrical radial (10) rings, with an equal thickness. The areas are given in Table. The fuel and bypass, described in the neutronics input by their flow area, have a special meaning for the reactivity parameters. The void fraction used for the core reactivity parameters is calculated according to the Equation 5.

$$\alpha_{ne} = (A_{ch}\,\alpha_{ch} + A_{bp}\,\alpha_{bp}) / (A_{ch} + A_{bp}) \qquad (5)$$

Table 4. *Most important neutronics parameters in the GENFLO input.*

Parameter	Value	Parameter	Value
Number of axial nodes	25	Area fraction of rings	.01, .03, .05, .07, .09, .11, .13, .15, .17, .19
Number of radial rings	10.0		
Axial nodes with control rods	1-5		
Radial rings with control rods	10	Temperature profile, K	1600-2100
Core height for neutronics, m	3.68	Local burnup, MWD/kgU	8 - 20
Core radius for neutronics, m	1.94	Fuel type	top 2, bottom 1
Channel area, cm^2	100.8	Void history profile, %	0 - 60
Bypass moderator area, cm^2	DF=0/ 42.4		

3.3. THERMOHYDRAULIC PLANT DATA

For the BWR plant the vessel geometry is described in the code by defining the average data for macro sections and flow connections between sections. A schematic presentation for the vessel in presented in Fig. 8. In core the number of axial nodes and number of radial rings is same as in the neutronics model. The system creates automatically the thermohydraulic nodalization based on the given lumped section data, which includes the number of calculation nodes. Flow paths, junctions, connect the nodes and inside sections e.g. the junction area is the same as the section area. The connections between sections may include flow area contractions and additional flow friction.

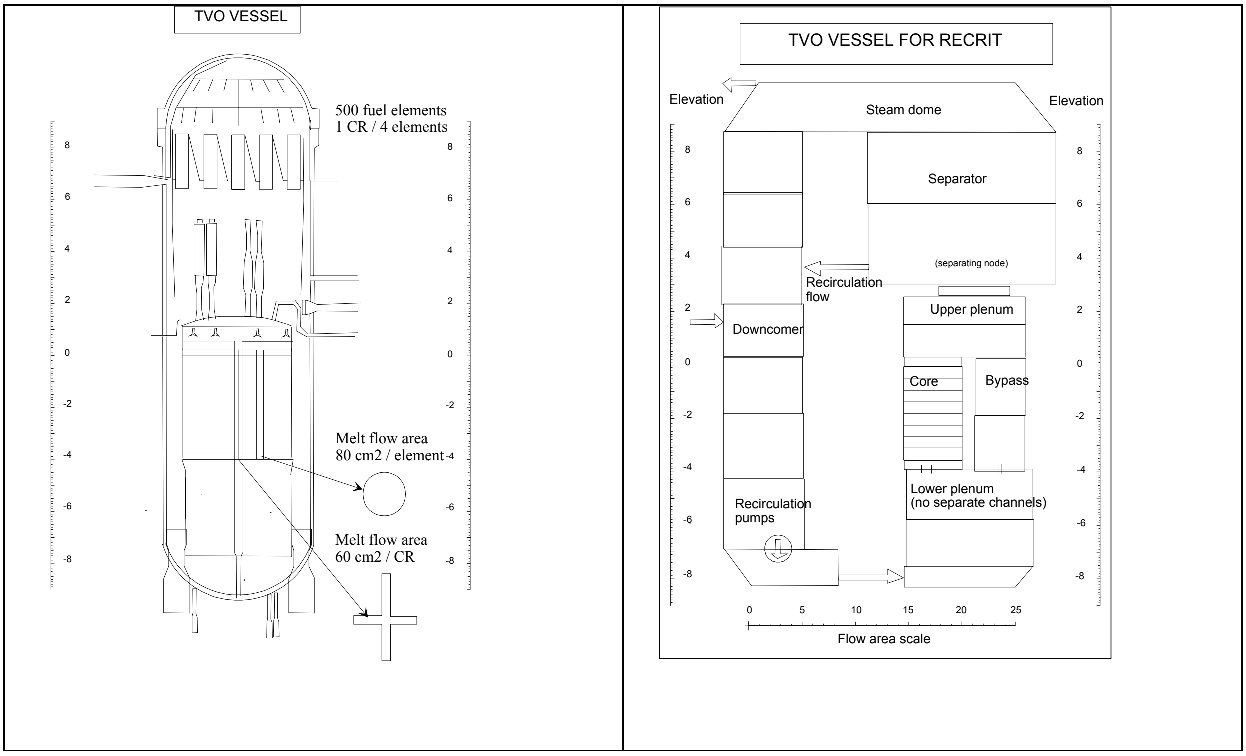

Figure 8. *Relative flow areas between different sections in the BWR plant and the vessel geometry with proper dimensions.*

Initial data for the full transient simulation and for benchmark cases are given in different ways. For the full transient run the coolant and fuel temperatures are initiated close to the saturation temperature at nominal conditions. The pressure in the beginning is nominal. But when initiating for the dry core situation, the coolant and the fuel temperatures and the void fractions are initiated according to the given initial distribution.

The steam line relief valves are used for different purposes in different simulations. One valve maintains the system pressure at 70 bar or at 5 bar for the benchmark case. One valve is needed for the ADS description and one as the steam line safety valve.

The pressure vessel is depicted in Fig. 8. The sections in the GENFLO nodalization is displayed in the right side of the picture. In Table 5 the most important paramaters, affecting these analyses are listed. A deficiency on the GENFLO model is that it does not divide the lower head divided into CRGT and lower plenum sections. In addition to that the flow connection into the bypass is on the core support plate level, not on the bottom of CRGT's. In the real plant the flow into the bypass channel is conducted by holes through the bottom of the CRD tubes.

Table 5. *Most important thermohydraulic parameters in the GENFLO input.*

Parameter	Value	Parameter	Value
Core area, m^2	4.2	Lower plenum height, m	4.58
Bypass area, m^2	4.0	TH timestep, s	0.005-0.05
Lower plenum area, m^2	12.0	C_o in drift flux model (-)	1.2
Downcomer area, m^2	11.0	V_{gj} in drift flux model (m/s)	1.0 / 4.0
Core height, m	3.68	Heat transfer dials	Recommended
Core inlet area, m^2	1.00	N.o. upper plenum nodes	3
Bypass inlet area, m^2	0.06	N.o. separator nodes	3
N.o. axial core nodes	25	N.o. lower plenum nodes	10
N.o. radial core rings	10	N.o. downcomer nodes	25
N.o. bypass nodes	25	N.o. dome nodes	5

4. RECRITICALITY BEHAVIOUR WITH ECCS STARTUP

4.1. SIMULATION OF THE FULL ACCIDENT SCENARIO WITH GENFLO

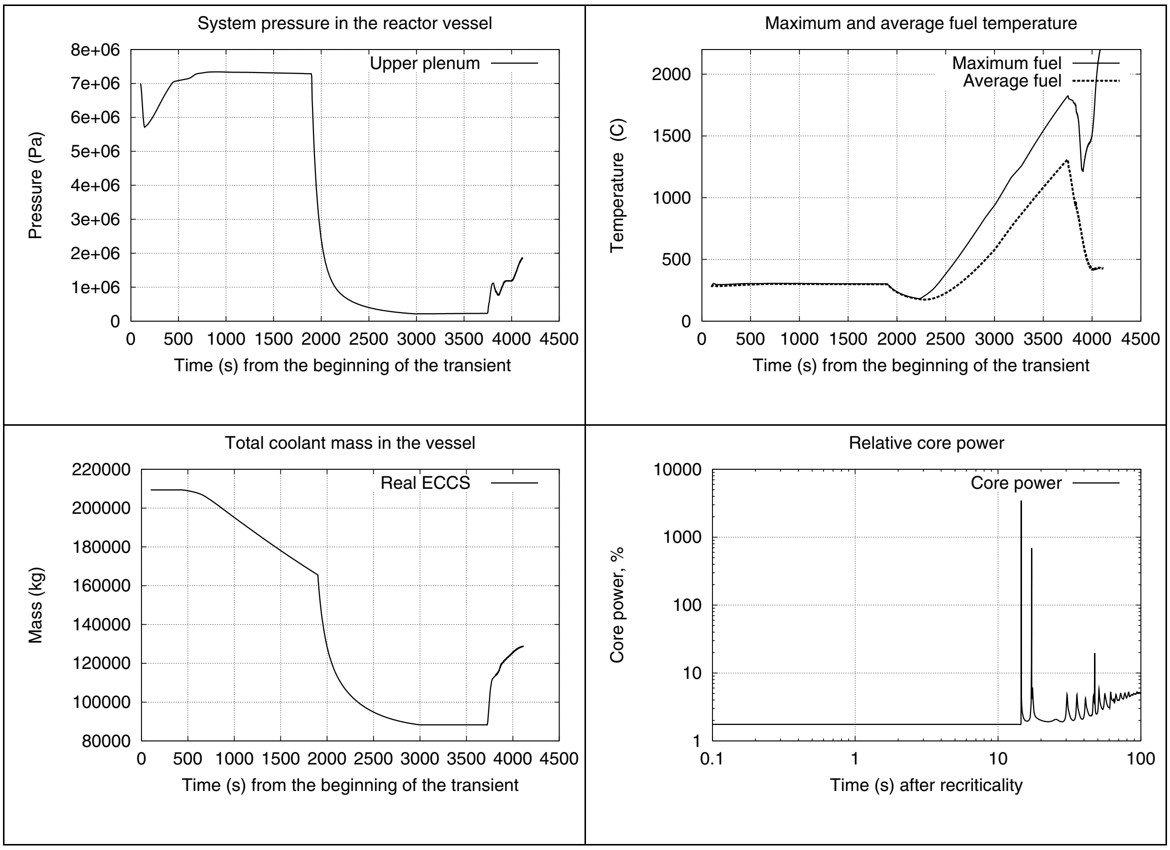

Figure 9. *GENFLO calculation results for the whole blackout accident ending with the core recriticality.*

The results in this chapter demonstrate that GENFLO can reasonable well simulate the whole period of the blackout transient up to the core recriticality. The entire recriticality transient calculated by the EU SARA project is presented. Fig. 9 depicts the BWR system behaviour after the blackout initially, and delayed ECCS start. The system pressure is maintained constant until the vessel level has dropped below the ADS initiation at 1800 seconds. The ADS depressurises the system below 10 bar. Because the LPCIS (and HPCIS) fails to start, the coolant inventory continues to reduce. After the core heat-up begins, radiation transmits heat from the core to the control rods. As soon as their temperature exceeds the eutectic melting temperature 1050 ^{o}C relocation of control materials to the bottom of the bypass zone begins.

4.2. CALCULATION RESULTS FOR THE BENCHMARK CASES OF THE SARA PROJECT

The three codes used in the SARA project SIMULATE, APROS and RECRIT could not be compared for the complete accident scenario. Instead a simplified scenario was defined, where the reactor core was assumed degraded according to the MELCOR result. Initial multidimensional profiles were defined for the fuel temperature, coolant temperature, void fraction and distribution of the control rods. The water level was initially at the top of the lower plenum and at the time 0.0 s the emergency injection was switched on. The system pressure was defined being constant 5 bar. Three injection rates were considered, the 160 kg/s (HPIS), 540 kg/s (HPIS + LPIS) and 1350 kg/s (AFW).

The reactor response in the similar scenario was studied with GENFLO as well, but with the new injection rates, 150 kg/s, 400 kg/s, 1000 kg/s and 3000 kg/s. The last injection is outside the normal injection capacity, but the test was needed for the developmental assessment. SARA comparison calculated recriticality due to delayed ECCS operation. It was considered as a well defined test case for the new features included in GENFLO.

In the GENFLO model the system pressure is not constant, and thus the system pressure results in Fig. 10 only indicates, how much deviations the pressure control system creates for different steam productions. The result for the reactor power shows that the prompt power peaks occur 190 s, 150 s, 60 s and 30 s after the reflooding start. The results for the average and maximum fuel temperature indicate that by two lower injection rates the core is cooled down continuously, even if the core is critical. All injected water is boiled off finally, but no local core temperature excursion takes place, when injection is continued. By two higher injecitons the local fuel temperature excursion cannot be avoided, however.

The average core temperature rise at the time of the first recriticality was used for the estimation of the possible fuel disintegration. It is essential to note that the highest fuel pellet enthalpy rise cannot be seen for the results for the maximum fuel temperature. This is simply due to the fact, that the maximum local power is not in the location of the maximum fuel temperature. Maximum core temperature shows values close to the melting points with the two higher injection rates.

In spite the fuel temperature excursion the average void fraction of the core drops down continuously The average void fraction is stabilized close 0.6.. By higher injections the core power profile is strongly peaked and the Doppler effect is not sufficient for damping the local power generation. Another fraction is defined for the critical core. It proves that the initial prompt power excursion takes place when 30 % of the core volume has $k_{inf} > 1.000$.

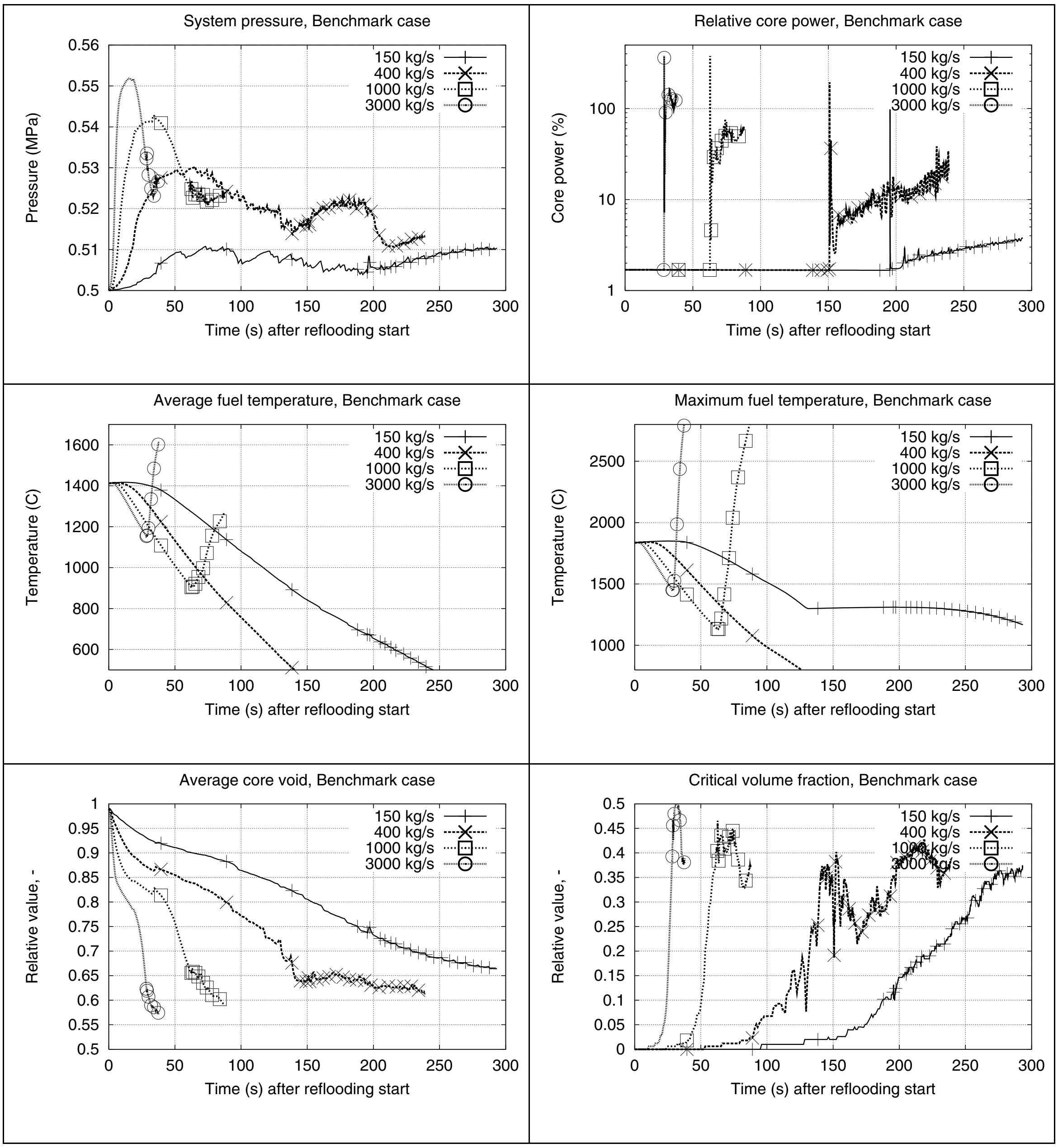

Figure 10. *GENFLO comparison for the benchmark test results after reflooding start.*

The total coolant mass and integral of the injection and outflow are shown in Fig. 11. The result indicates that most of the injected water remains in the reactor vessel in the calculated variations. This means that the situation is not well stabilized at the end of the calculation. The energy balance contributions are for the total energy, energy input into the core and injection, and the energy flow out. The system energy balances include the total energy content in the fuel, the energy input due to the neutron and decay power and the energy flow out through the relief valves. The balance defined as energy content – energy input + energy outflow was maintained during the calculation. The total energy results show two trends. By low injection rates the core is cooled continuously. By larger injection rates the energy content increases after the recriticality and cannot be controlled.

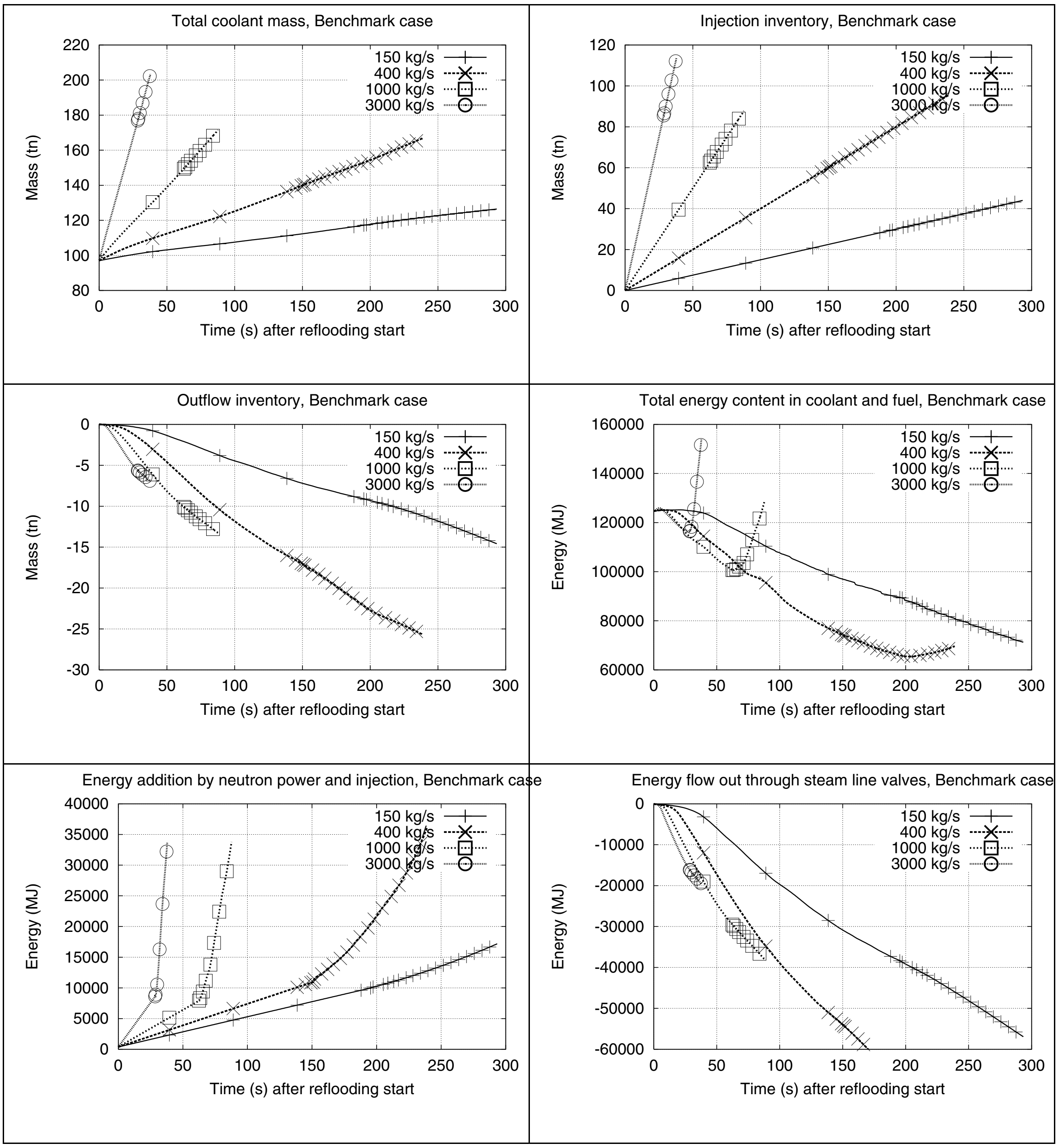

Figure 11. *GENFLO comparison for the benchmark test cases after reflooding start.*

The result for the core mass flow in Fig. 11 indicates, that even if the injection is into the lower plenum, it takes some time before the core inlet flow equals the injection rate. The injection is forced into the vessel itself, but the injection into the core results from the gravitational level differences mainly between the downcomer and fuel channel. After the reflooding water enters the core, steam generation creates the pressure difference, which forces the downcomer water level higher than the core water level. When the level difference is high enough, the core inlet flow equals the injection rate. No boiling occurs on the downcomer, thus gradually all injected water is channelled into the core inlet.

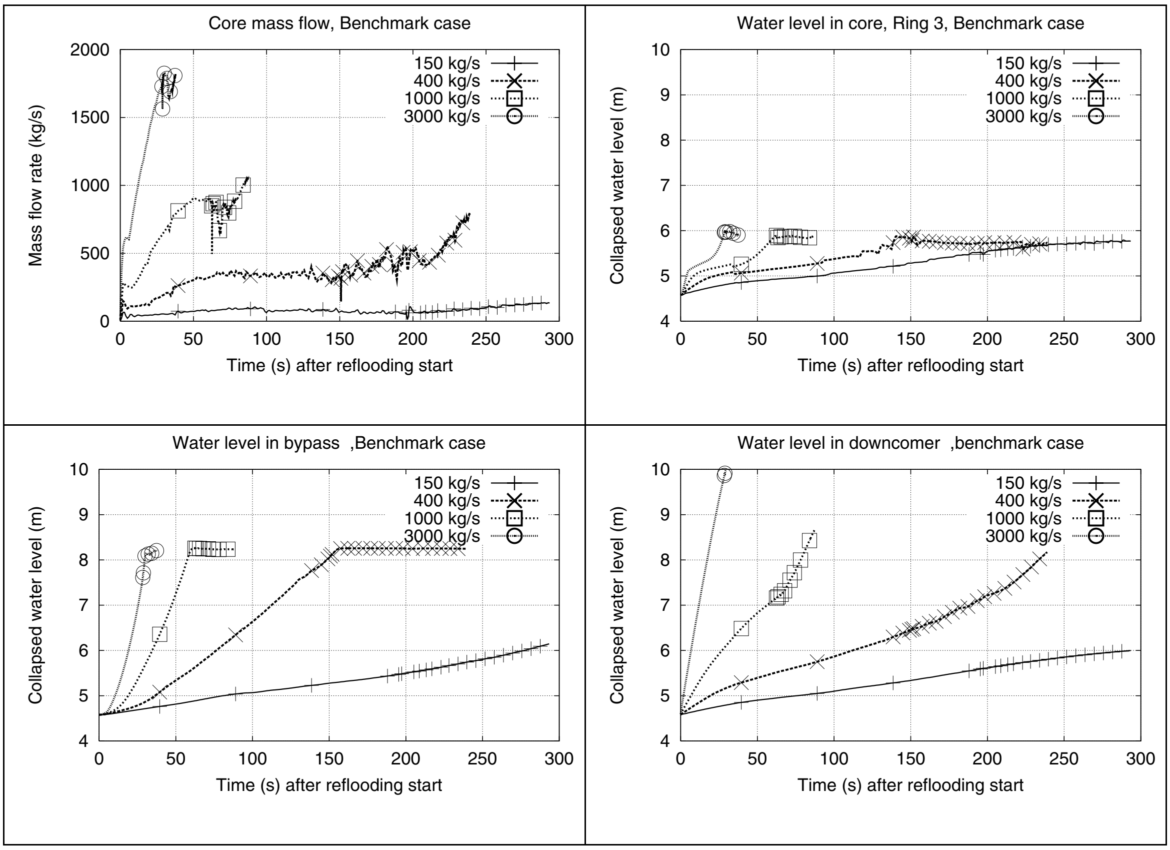

Figure 12. *GENFLO comparison for the benchmark test cases after reflooding start.*

The water levels show clearly, that the reflooding process is a gravity driven process from the core point of view. With low injection the collapsed levels are about the same. With 400 kg/s already an extra level is needed on the downcomer side.

Results for the effective multiplication factor and the relative core power are shown in Fig. 13 on the logarithmic scale fixed to the time point of the first recriticality. The result for the effective multiplication factor shows the rise above the prompt criticality limit (1.006), short drop after the first recriticality and later the variations during the non-prompt power generation. The result for the core power generation shows the relations between the prompt power peak and the power generation after that.

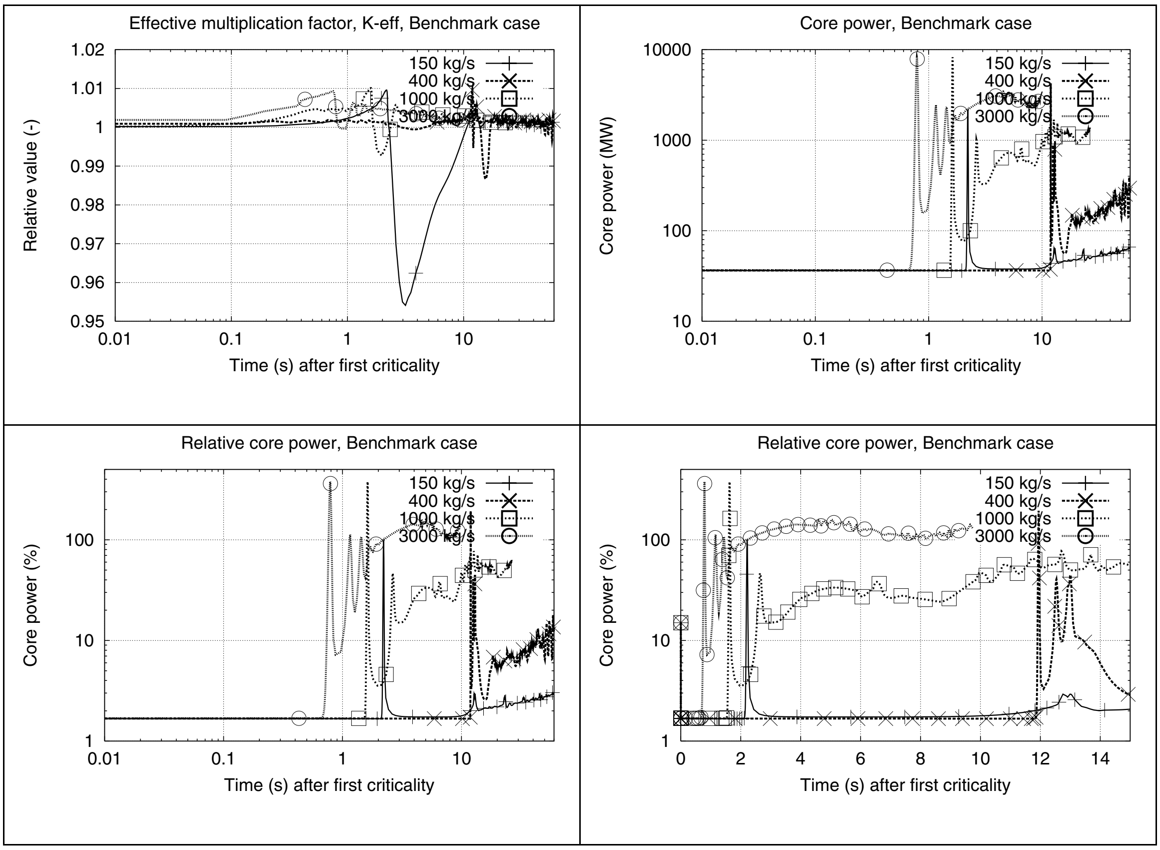

***Figure 13.** GENFLO results for the period after reaching the recriticality first time.*

The results of variations are analysed with the same procedure, as was done in the SARA project in Table 6. The relative power peak is referred to the nominal reactor power. The result shows clearly that the prompt peak duration is really short. The higher injection rates perhaps include so many oscillations that their first power peak is less energetic than that of smaller injections just in this analysis case. The normal heat transfer from the fuel rod to the coolant is too slow for controlling this power peak. The key mechanism is the Doppler effect in the fuel, even if later on it not efficient enough to prevent the continuous power increase.

The model included the feature that 2.5 % of the neutronic power generation is directly absorbed into the coolant. The power absorption is used directly for the evaporation of the liquid. This evaporation takes place immediately in the model, even if the delays are typically related to the flashing process. Without this the prompt power peaks would be much more efficient. In the analysis the bypass level was higher than the core level. Because the effect of the bypass void was not considered in the reactivity parameters, and the collapsed water level there was higher than in the core, the analyses can be considered non-conservative.

The process for evaluating the maximum energy deposition into the fuel pellets needs additional calculation. The code does not include any core wide follow-up for the energy deposition. Instead the calculation is based on the average energy stored into the fuel and local peaking factor. The assumption is that (maximum power deposition into fuel) = (average power deposition) * (maximum power peaking). For the fuel integrity analysis the critical parameter is the maximum energy deposition into the pellet per unit mass. The result shows clearly that in these variations the energy deposition does not exceed the limiting value for the energy deposition into the fresh fuel (170 cal/g) neither the maxim deposition after the long burn-up (65 cal/g).

Table 6. *Comparison the results from GENFLO.*

Case No:	1	2	3	4
Constant injection kg/s Time at first power peak (s)	150 190.	400 150.	1000 60.	3000 30.
Peak amplitude, relative	0.63	1.52	2.87	3.32
Total peaking factor (-)	10.31	6.75	5.50	5.80
Duration of 1:st peak (s)	0.13	0.10	0.09	0.09
Half width of 1:st peak (s)	0.045	0.024	0.016	0.016
Total energy in the peak (MJ)	145.	450.	326.	305.
Average energy addition (J/g)	1.41	4.68	3.18	3.00
Max. energy deposition (J/g)	14.9	31.6	17.5	17.4
Same as cal/g (1 cal = 4.2 J)	3.34	7.5	4.17	4.14
Power at end of simulation	.04	.40*	.60 *	.60 *
Time at end of simulation (s)	290	180.	70.	70.
Max. FT at first recriticality (C)	1350	750.	1200.	1200.
Max. fuel temperature (C)	1800	2800	2800	2800
Max. FT at end (C)	1100	2800*	2800*	2800*

*) End time of the simulations means time, when the maximum temperature of fuel reaches 2800 ^{o}C.

The scoping study made with the same methodology, as the recriticality analyses in the SARA project, pointed out some uncertainties, which means that the calculation results are conservative and partially non-conservative:

1. From the bypass void fraction no effect was calculated into the neutronics parameters. In this case neglecting effect made the analyses non-conservative.

2. The new Atrium fuel includes a water space replacing 3 x 3 fuel rods. It perhaps allows water to rise faster than the quenching front propagates. Because the water space was not considered, the analysis results can be considered non-conservative.

3. The direct heat absorption into the coolant was defined as a prompt process. With a power peak exceeding the nominal core power the prompt additional flashing reduces effectively the power rise. From the thermohydraulics it is known that flashing has a time delay. The rapid time dynamics of this flashing should be studied more. If the flashing term due to the neutron power is too prompt, even this feature makes the present analyses non-conservative.

4. On the basis of the old RECRIT thermohydraulics, an additional core inlet friction was used in the input of the new run. The old RECRIT needed this for balancing the oscillations. It is needed any more in GENFLO. Thus it may be that the core inlet flows

by larger injections were somewhat underestimated in these analyses. The possible extra friction makes the analysis results non-conservative.

5. The result for higher injections was the rise of the core maximum temperatures if the injection is continued after the prompt power excursion. The heat transfer model should be studied further in order to see, if the post-dryout heat transfer is underestimated in the model. The possible weak heat transfer can be seen as an over-conservative feature with respect to the fuel temperature.

These uncertainties were not studied further in this study. A part of them were recognized already in the RECRIT contribution into the SARA project, but because the uncertainty analyses were not considered actual with other calculation models (SIMULATE-3K, APROS), the uncertainty study with RECRIT was not included in SARA.

5. BOUNDARY CONDITIONS FOR THE MELT RE-LOCATION INDUCED REFLOODING

5.1. MELT RELOCATION INTO THE LOWER PLENUM

The analysis methodology in this chapter has been formulated by Sehgal and Dinh (Sehgal & Dinh 2002).

The material properties of the core material are presented in Fig. 14. The relevant numerical data for evaluation of the FCI scenario has been collected in Table 7. In Fig. 15 some geometrical details have been clarified.

Table 7. *Main dimensions affecting to the relocation of the molten control rods and steam explosion in the lower plenum.*

Parameter	Value	Parameter	Value
Vessel inner radius, m	2.770	Thickness of the CR blade, m	0.008
Barrel inner radius, m	2.035	Breath of a CR wing, m	0.132
Barrel wall thickness, m	0.025	Active length of CR, m	3.646
Total lower plenum height, m	5.192	Total length of CR, m	3.942
Bottom curvature radius, m	2.770	B_4C holes in a single CR wing	456
Area of the reactor barrel, m^2	13.01	I.D. of a CR hole	0.006
Length of CRGT tubes, m	3.732	Depth of a CR hole, m	0.114
I.D. of CRGT tubes, m	0.290	B_4C mass in a single CR, kg	10.4
O.D. of CRGT tubes, m	0.296	Total weight of a CR, kg	134
Area of a CRGT tube, m^2	0.0683	CR area, cm^2	42.4
Number of CRGT tubes, -	121	CR path thru support plate, cm^2	60.
Fluid area of CRGT tubes, m^2	8.26	GB CRGT area, m^2	7.75
Lower plen area w.o. CRGT	4.46	GB CRGT length, m	3.66
Pitch between CRGT tubes, m	0.3075	GB CRGT inlet area, m^2	0.0770
Fuel inlet area, cm^2	78.5	GB Core inlet area, m^2	0.991
B_4C total mass, tn	1.26	GB downcomer area, m^2	9.31
Steel total mass, tn	14.9	GB core area, m^2	5.37
Core support plate thickn. m	0.082	GB bypass area, m^2	4.1
Channel weight, kg	27	GB CRGT volume, m^3	28.5
Channel material	Zr-4	GB lower plen volume, m^3	26.7

Melting of the 3 m content (80 %) of the control rod blade material produces 11.9 tn of steel. If the melt fills only the bypass area in the vicinity of fuel elements (500 * 0.004238 = 2.12 m^2) the steel is filling 0.81 m in the bypass section. Additionally 1.26 tn B_4C is filling 0.24 and the total melt pool is 1.05 m in the bypass zone. In MELCOR analysis these inventories were 13 tons of steel and 1.1 tons of B_4C. The mixture density of the steel - B_4C is 5910 kg/m^3.

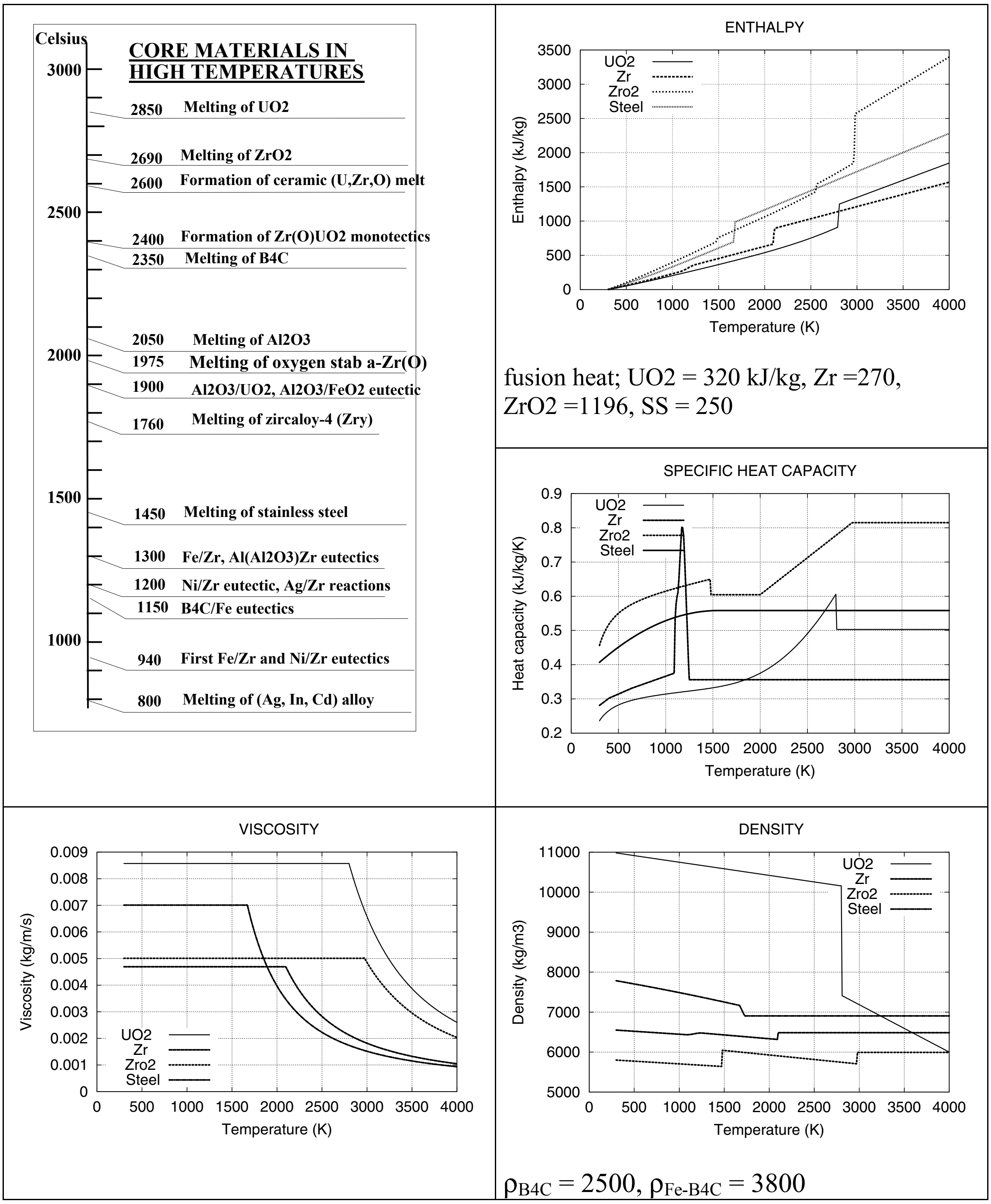

Figure 14. *Core material characteristics at high temperatures.*

The geometries of the vessel, CRGT, control blade, fuel bundle and the associated locations and flow areas are important in determining the control rod melt discharge to the water in the lower head.

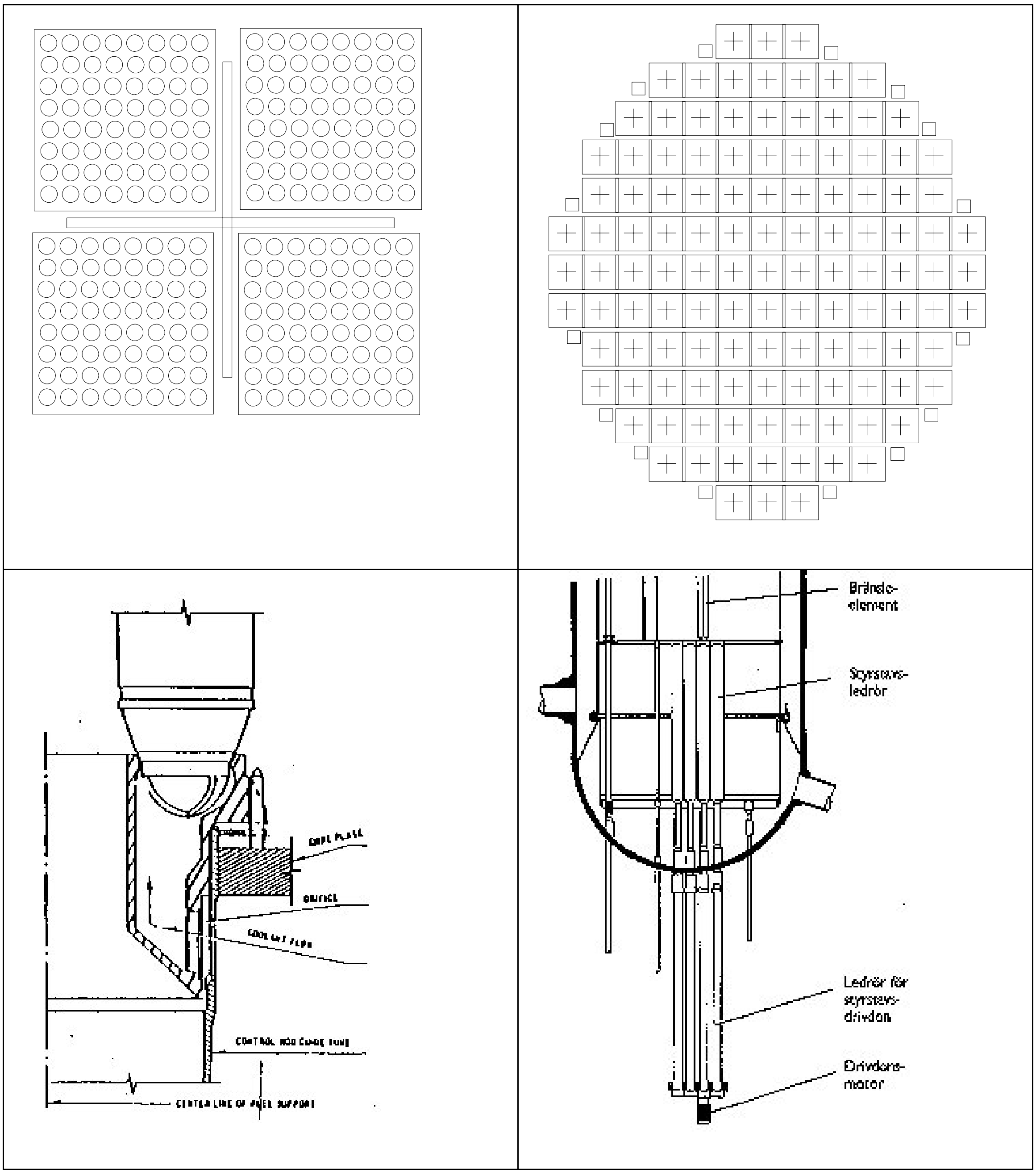

Figure 15. *Fuel element with the control rod crucifix and the core loading structure.*

Fig. 15 shows the principal structure of the fuel elements around the crucifix control rods, the loading arrangement of the core, inlet pathway into the fuel element and the lower structures in the lower plenum. The schematic picture of the pressure vessel and the volume distribution behind the GENFLO nodalization were presented earlier in Fig. 8. 121 CRGTs, with O.D. 0.296 m and pitch 0.3075m exists in the lower head. An instrument tube is located between four CRGTs. The flow area of control rod is 0.0048 m^2, but the crucifix shaped hole in the bypass is 0.0060 m^2. The melt can be ejected through this hole into the water filled CRGT. The assumption is this case is that the thin walled (3 mm) CRGT is broken and the melt contacts the lower plenum as well. No hole ablation will take place during the melt release since the melt temperature is lower than the melting point temperature of the structural steel.

The other pathway for the control rod melt flow is through the coolant orifice in the rod bundle whereby it can reach the water in the lower head. The flow area for this pathway is 0.0078 m^2. However, the melt has to eat through the Zircaloy shroud

The initial velocity of the melt flow into the lower plenum may be defined from the Bernuolli equation $v = \sqrt{2hg}$ for the 1.05 m metal pool as 4.53 m/s initially. In Fig. 16 the melt release has been demonstrated by Fluent calculations. The metal viscosity is 10 times above that of water, and thus the wall shear has only a little effect on the flow profile. In this way no additional results can be achieved from the Fluent simulation. The gravitational forces accelerate the falling melt and the velocity in the free fall as a function of the falling distance is $v = v_0 + \sqrt{2gs}$ m/s. The initial mass release through the 60 cm^2 hole is 160 kg/s and through the 78 cm^2 hole 209 kg/s. In the next the 200 kg/s release is assumed. The respective enthalpy flow is 200 MW, corresponding to the maximum boiling capacity of 125 kg/s.

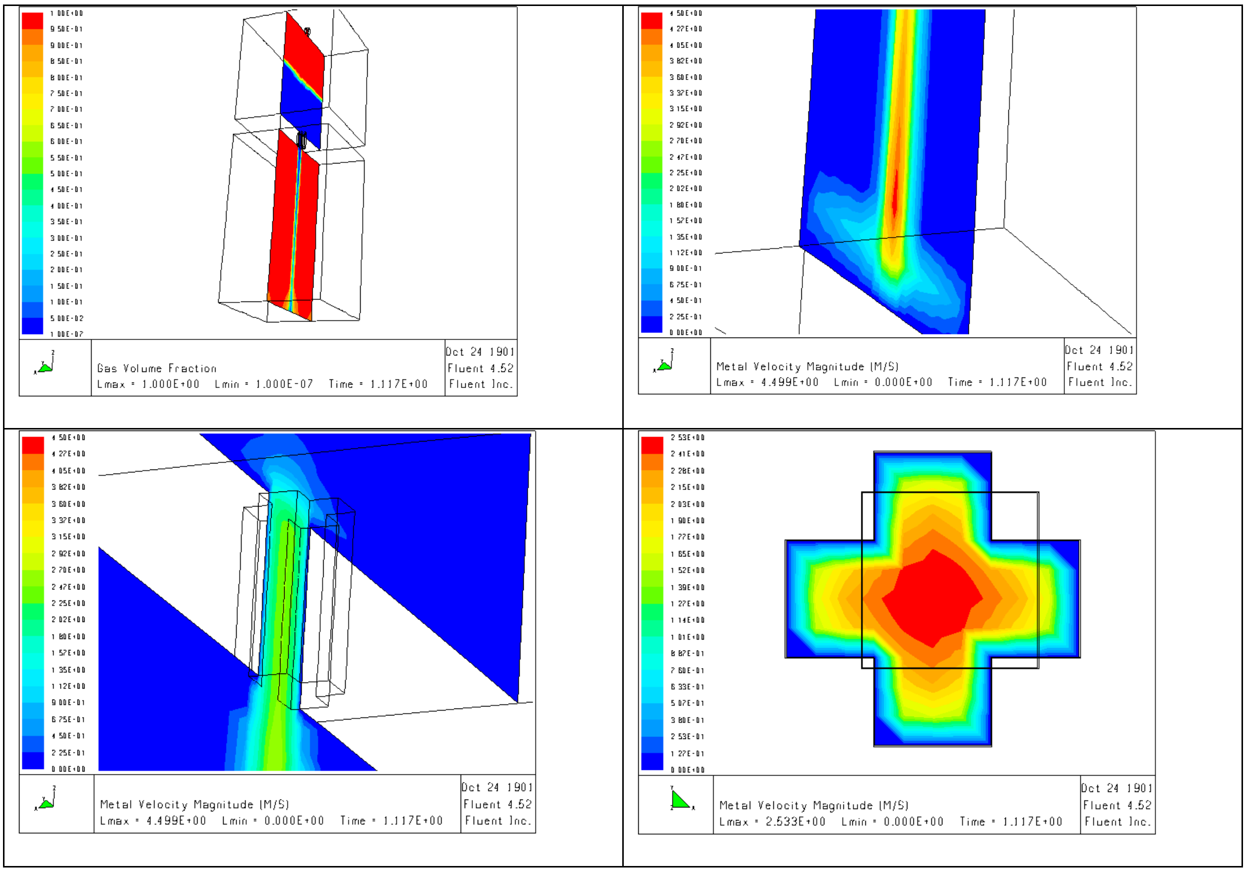

Figure 16. *Results from the Fluent calculation.*

For the fuel coolant interaction three different scenarios were assumed, described in (Sehgal & Dinh 2002): a. melt does not fragment, b. melt fragments, no steam explosion, steam production only and c. melt fragments, a steam explosion occurs.

The falling melt along the whole length has the area of 1 m^2.Without fragmentation, by assuming the pool boiling critical heat flux 1 MW/ m^2, the melt creates only 0.625 kg/s boiling. Thus melt fragmentation is required for effective level swell. This scenario is considered in next chapters.

5.2. NON-ENERGETIC SCENARIO

The analysis methodology in this chapter has been formulated by Sehgal & Dinh (2002).

The estimated melt release of 200 kg/sec means that the melt is deposited to the lower head in > 70 seconds. During this period the melt-water interaction process in the lower head will produce steam, whose upward flow will reduce the melt drop rate. The melt jet of ~9 cm diameter enters the water pool at 5-6 m/s. The break-up length can be estimated by Saito correlation, which results in 1.2 m. Since the melt relocation, most probably, is in the central region, a significant fraction of the jet will fragment into droplets. The situation is very similar to the FARO experiments for saturated water pool, which show the typical droplet size d_p = 3-5 mm. The premixing zone (melt-coolant interactions) is about 1 m in diameter and goes down from the water surface to the pool bottom. The mixing volume of approximately 3 m^3 can be envisioned.

The heat transfer from the melt to coolant can be evaluated from the radiative and the film boiling components. For emissivity of 0.45, the radiative heat flux is calculated to be 200 kW/m^2 for 1700 K; and the film boiling is 270 kW/m^2. In sum, the heat removal is much less than the CHF value of 1 MW/m^2. Note that in the pool, the melt temperature cools down so the heat flux goes down to 300 kW/m^2, i.e. essentially film boiling, since the temperature remains greater than the minimum film-boiling temperature.

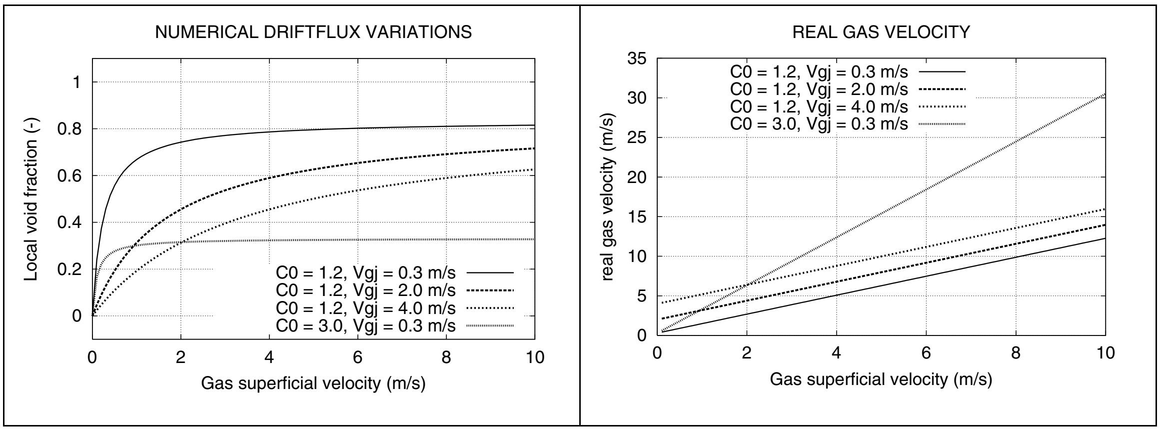

Figure 17. *Results from the drift flux numerical variation*

Due to heat transfer the level swell in the lower plenum can be expected. The problem is how the complex geometry with CRGT's behaves in this situation. In calculation models it is a question of the selected drift flux correlation. Fig. 17 illustrates the situation. The drift flux correlations, e.g. the EPRI correlation are valid for 1-D, narrow channels, and after calculating the values for typical PWR geometries (diameters 0.015 – 0.5 m) the representative drift-flux parameters for this correlation are C_0 = 1.2 and V_{gj} = 1.0 m/s. In a single tube the values C_0 = 1.2 and V_{gj} = 0.3 m/s are well representative. In the annular geometry the values C_0 = 3.0 and V_{gj} = 0.3 m/s give the best result on a large gas flow rate. In this result the geometry wide circulation has its effect on the parameters. The relationship between different approaches has been illustrated in Fig 17. The void fractions for the smaller geometries may rise rather high by increasing steam productions. The results for the annular geometry show rather soon a saturated value. The complex geometry with CRGT's may resemble that of annular geometry for the phase separation point of view. In the annular geometry the existence of gas creates a vessel wide circulation, which makes the phase separation very effective. No one of these approaches was selected directly for the lower plenum phase separation in GENFLO. As a compromise C_0 = 1.2 and V_{gj} = 4.0 m/s was selected, which is according to Fig. 17 between the EPRI and annular geometry results.

Based on the estimations for the degree of fragmentation, Sehgal and Dinh (2002) estimated that the steam flow through the core would be 8m/sec. Additional conclusions were that the void fraction for the coolant entering the core would be 30 % and the overall core reflood swell level would be 0.33 m. The 30 % void comes from the assumption of the boiling on the bottom of the core. Because this is calculated by the code, it was not considered as a boundary condition Considering level swell the following approach was adopted: the steam generation producing 8 m/s steam flow is initiated into the lower plenum abruptly, and as a consequence of it the water has to escape from the lower plenum to the core and downcomer. The initial level is varied in order to find the limit, when the reactor becomes critical, and when not. The level variation gives information of the maximum possible power excursion.

5.3. ENERGETIC SCENARIO

The analysis methodology in this chapter has been formulated by Sehgal and Dinh (2002).

The melt poured into water is fragmented and in the first stage the coarse fragmentation is expected producing the particles in the 1 - 10 mm cm size. Already the cloud of droplets can create strong boiling, which was used as the boundary condition in the previous chapter. The droplet should not solidify as the coarse fraction, instead the fragmentation should continue into the atomization degree, where the particle size is less than 1 mm. If this process is fast enough, heat can be released into the coolant with such a speed that the thermal energy release can be considered as explosive. The void fraction in the vicinity of the melt should not be too high before the final fragmentation into the small particles.

The final fragmentation is typically a consequence of the chain reaction. An initiating event, called triggering, occurs, e.g. when the molten metal hits the bottom of the facility. After triggering the propagation for the steam explosion may be uncertain. A chain reaction, where new explosions are triggered by earlier ones, is needed for the real steam explosioin effect.

Results from different attempts to quantify the probability of the steam explosion and its energy conversion ration have been described in Fig. 18.

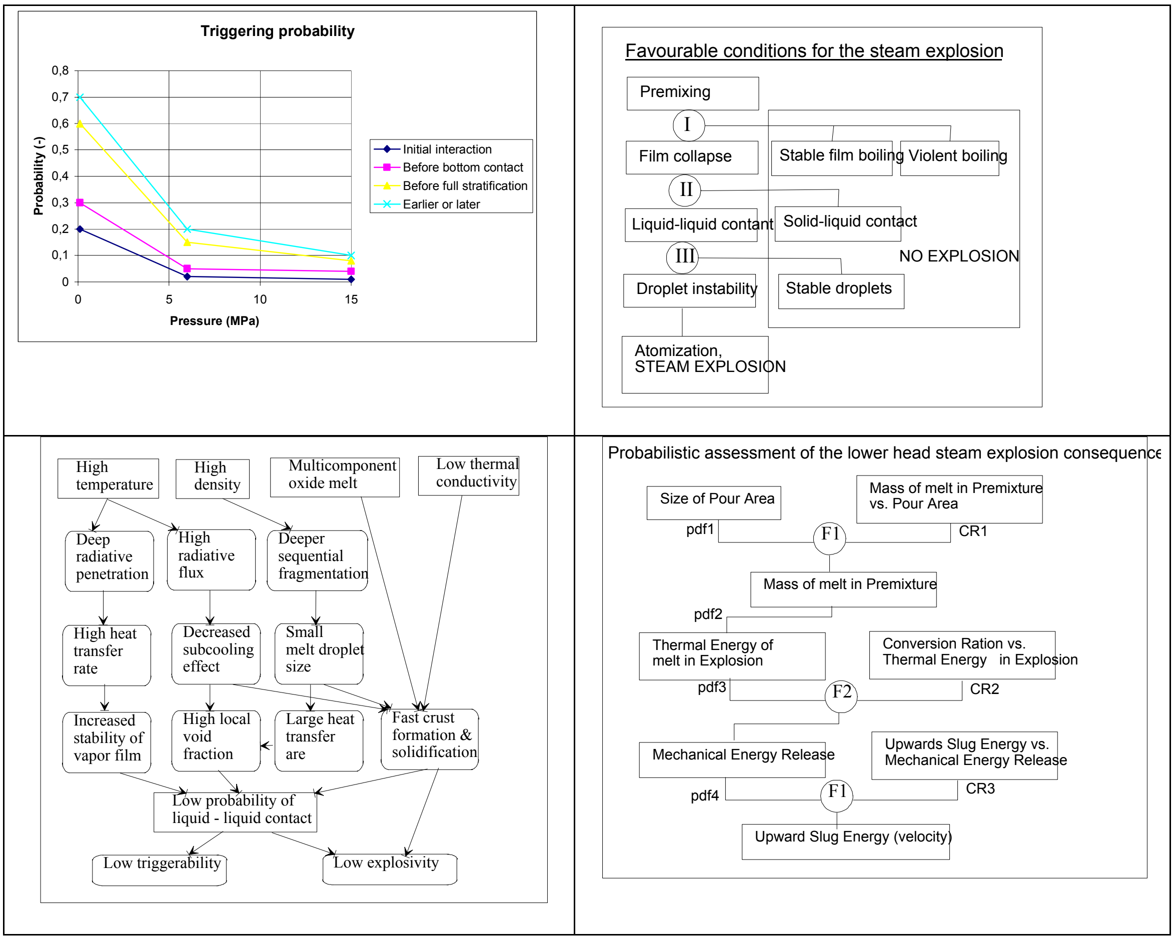

Figure 18. *Triggering probability estimated in different approaches.*

Large-scale experimental programmes have resulted conversion ratios ranging from 0.3 % to 3 %. With the prototypic material, finely fragmented without subcooling, indicate a conversion efficiency of 4 % Based on the CHYMES prediction the upper bound efficiency for large pours is 20 % at early times in the pour, falling to approximately 8 % when vapour production becomes significant.

The amount of melt in the mixing zone is evaluated to be M = 1200 kg, i.e. it takes effectively 6 seconds for the melt to sediment in the pool. The heat removal rate is evaluated to be (Sehgal & Dinh 2002)

$$Q = 6\ q''\ M/(d_p\ \rho_m) = 120\ MW \tag{9}$$

The steam production rate is Q/h_{fg} = 55 kg/s or 50 m^3/s at 2 bar system pressure (pressure assumed by KTH, in previous SARA studies 5 bar was applied, for the level swell the volumtric flow is most important). This steam will vent through the core and the pump making the pump to work like turbine. Through the core, it will go into the fuel channels and unblocked inter-channel spaces. Given the cross-section area of the lower head is 15 m^2, the steam velocity is 3.2 m/s. For the core region, the steam velocity will be about 8 m/s.

Given the rate of energy supply to the pool by steel B_4C melt is 200 kg/s x 0.8 MJ/kg - 160 MW, only 75% of this is extracted during the premixing phase. The rest is stored in the melt/debris accumulated on the lower head bottom. For steel latent heat (0.32 MJ/kg) and specific heat (0.4 kJ/kg.K), this 75% heat extraction indicates that the melt is solidified, and cools down from 1700 K to about 1000 K.

From the FARO experiments, as well as from results of premixing analyses, it can be seen that the level swelling is about 0.5 to 1 m for small pool (FARO), and far less in the large diameter BWR lower head. In fact, given the premixing zone volume of 3-4 m^3 with its effective void fraction of 50% the level swell in the core area (cross-sectional area of 12 m^2) will be ~0.3 m.

Based on these considerations we will postulate that the control rod melt which is primarily steel, would undergo energetic MCI. It should be recognised again that the initial conditions for the control rod melt are not conducive to an energetic steam explosion due to very low superheat of the melt. Nevertheless we will postulate that a steam explosion would occur.

We will deal with 200 kg/s of metallic melt delivered to the water pool. We consider a steam explosion in the lower plenum. To maximize the impact of a steam explosion, we assume that the explosion was triggered after the first melt already reached the water pool bottom (e.g., triggered by coolant entrapped in the melt). This way, a substantial melt amount has accumulated in the premixture. With the initial jet velocity of the order of 5 m/s, and considering the reduction in the melt velocity in water, the melt reaches the pool bottom within 2 s, leaving about 400 kg of melt in the premixture. Since the water is saturated, a highly voided premixture is expected, which reduces the explosion energetics very significantly. In fact, taking a highly conservative conversion ratio of 15% of a thermal energy of 320 MJ (0.8MJ/kg molten steel relative to water saturation temperature), the mechanical energy of 48 MJ could be released in the explosion.

Due to the explosion venting, no significant water amount would be pushed upwards by the explosion at the very location of the premixture. Instead, the explosion may cause the water pool to slosh, pushing the pool coolant to penetrate into the core. The water is of very low compressibility, so the process is essentially isochoric. More precisely, the coolant pool's volume shrinks due to the high pressure generated in the explosion, which causes the steam in the premixing zone to condense.

A maximum volume that could form a "slug" is estimated to be of the same volume as that of the premixing zone (V_{mix}). V_{mix} for an in-vessel MCI from a single jet situation can be conservatively bounded to V_{mix} = 3 m^3. Given the core fuel bundle cross-sectional area of 7.2 m^2 and the lower plenum area of 15 m^2, about half of V_{mix} (i.e. 1.5 m^3) may be pushed into the core through un-blocked pathways (in the fuel channels). The time scale for shock wave propagation and collapse of the premixing zone (L- 3 m, D- 1 m) is $L/c_{mixture}$ = 3 m/150 (m/s) = 7..20 ms. For the cross-sectional area of about 4 m^2 (2/3 volume is coolant and 1/3 are filled by the fuel elements) the slug penetrates into the core with a velocity of 20…60 m/s during a period of 7..20 ms, raising the water level to about 0.4 m. This volume will stay in the core even when the pool dynamics would favour liquid re-collection into the lower plenum. The reason is that the liquid receding now is resisted by evaporation, and not any more driven by the pressure wave as during the steam explosion that formed the slug in the first place.

Another conceivable scenario of slug penetration is when the pool sloshing is asymmetric and the slug penetrates only a half of the core's cross-sectional area.

The slug penetration parameters that can be used as coolant conditions for the recriticality analysis are listed below. Uncertainties in steam explosion assessment in complex geometries of the core and lower plenum necessitate a l range for these parameters. Based on this formulation four variations are proposed as the boundary condition of the energetic steam explosion calculation. In the two first variations the water slug penetrates the whole core cross-sectional area, and two penetration velocities are assumed, rapid and slow penetration. In the rapid penetration the slug velocity is 60 m/s and the penetration time is estimated as 7 ms. In the slow penetration the velocity of 20 m/s is assumed and the penetration time 20 ms. In two other variations the assumption is that only the half of the core is reflooded, the rapid penetration with 80 m/s velocity and the slow penetration with 20 m/s velocity. The rapid penetration time would be 10 ms and the slow penetration time 40 ms.

The boundary conditions defined by Sehgal and Dinh (2002) were considered so far as possible. The slug movement was created by an abrupt steam addition into the bottom of the lower plenum. Due to numerical problems to calculate the water movement due to the explosive energy release, a ramp of few milliseconds had to be applied in the beginning of the steam production, thus the length of the pulse was made longer than the specified one. The specifications included the definition for the water volume entering the core, the respective reflooding (cold water rise) level and the void fraction of the reflooding water. The volume was defined being 1.5 m^3, the reflooding height 0.8 m and the void fraction 0.0 %. The problem was approached in the inverse manner however. It was decided that the amount of the water entering the core will not be limited. Instead water is allowed flowing into the core until the recriticality conditions are encountered. From the result it will be calculated, how much water is needed for the criticality. The void fraction was not preset, neither. In reality the water penetration into the core is so rapid that no boiling can be expected.

6. GENFLO RESULTS FOR THE RECRITICALITY

6.1. MODELLING OF THE SPECIFIED CONDITIONS IN THE GENFLO CODE

The modelling principles with GENFLO have been discussed previously in the chapter 3. The proposed variations are listed in Table 8. The effect of the lower plenum swell and steam explosion boiling was described in GENFLO by injecting vapour into the second lowest node in the lower plenum. The second lowest node was needed in order to prevent the steam flow partially into the downcomer side. By all steam injections a short ramp was needed. The core inflow void fraction was not adjusted, it was given to be calculated by the code. The half symmetry injection was not possible to be modelled, because the neutronics described the core two-dimensionally. The variation was done, but by defining the half core as an inner circular section, not as the diametric half.

Table 8. *Recommended parameter variations for the steam explosion study.*

Parameters	Swell	EngFR1	EngFS2	EngHR1	EngHR2
Core steam flow rate, m/s	8	-	-	-	-
Void fraction in core inlet, -	0.30	0.00	0.00	0.00	0.00
Water slug velocity, m/s	-	60	20	80	20
Period of slug penetration, ms	-	7	20	10	40
Total coolant volume to core, m^3	-	1.5	1.5	1.5	1.5
Reflood height, m	0.33	0.4	0.4	0.8	0.8
Core inlet free for penetration	full	full	full	half	half

The parameter variations pointed out that the one-dimensional two-phase model easily overestimates the void fraction in the lower plenum type of pool, where the boiling heat source in located on the bottom. The lower plenum coolant expands efficiently, but on the other hand the calculated void fractions are higher than the expected, and the reactivity may be wrong. The topics was discussed in the previous chapter. The rapid volume expansion was evaluated unrealistic, and that is why the drift flux parameters were selected as V_{dr} = 4.0 m/s and the distribution coefficient C_0 = 1.10.

The case specifications included specific definite volumes for the coolant entering the core. Following the problem definition was found difficult for the GENFLO type of the code, because of which the problem was approached in an inversed way. The coolant volume was allowed to increase above the limit defined by Sehgal and Dinh.

6.2. CALCULATION RESULTS FOR THE NON-ENERGETIC FUEL-COOLANT INTERACTION

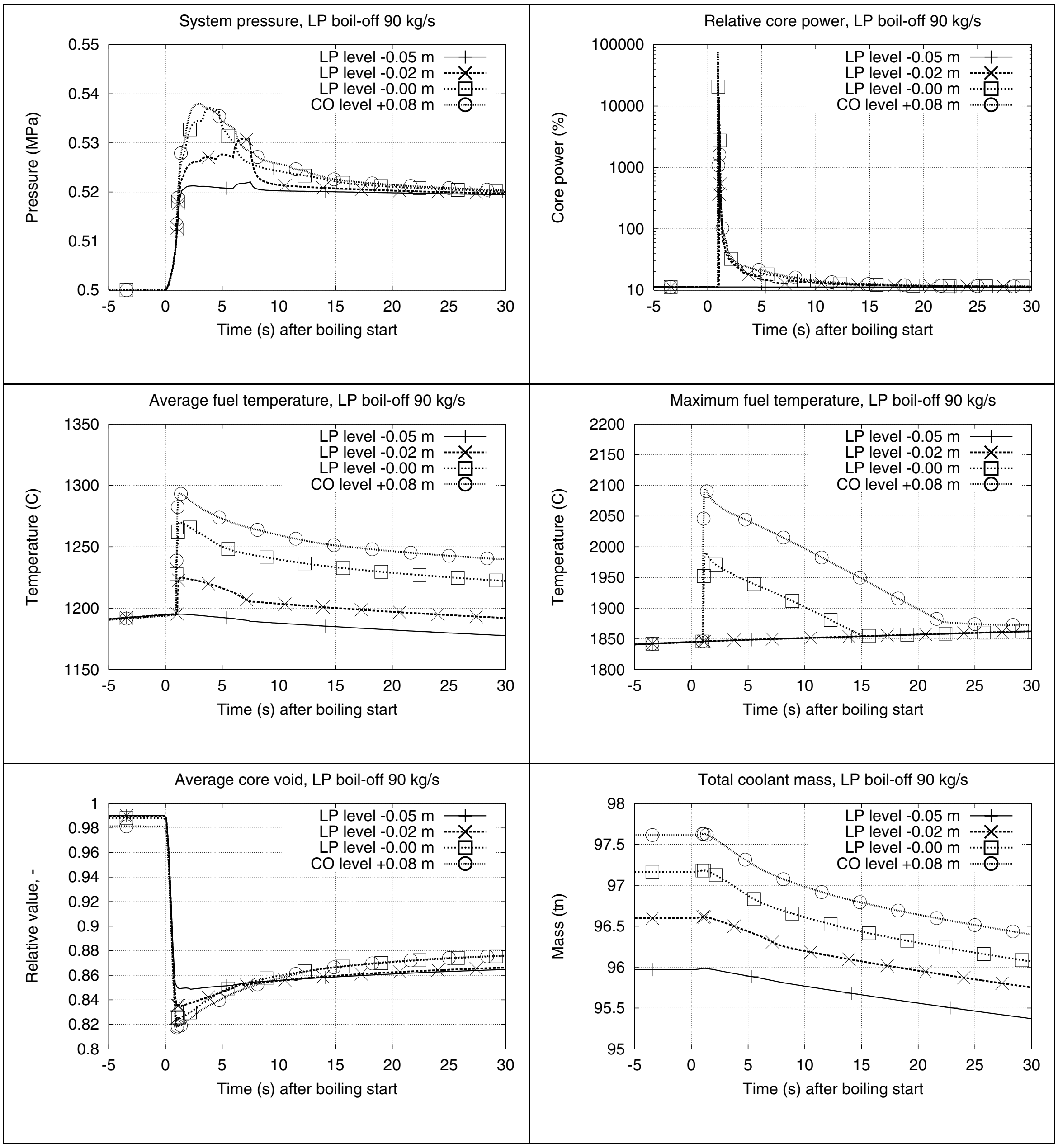

Figure 19. *GENFLO variation for the nonenergetic core flooding.*

The defined 8 m/s of steam flow rate was maintained, and injected into the lower plenum with the ramp of 0.1 seconds. The initial core level positions were varied between the non-critical case and maximal critical case. It was found that by initial lower plenum level, 5 cm below the core support plate, no criticality is produced in the core. In addition to that it was recognized, that if the initial water level was more than 8 cm within the core, the criticality effect was not further increased. That is why the parameter variation was simply spanned for the initial levels in the lower plenum -0.05, -0.02, 0.0 and 0.08 m with respect to the core support plate. The results of these variations are discussed here. In addition to this some reactor physical variations are presented in the chapter 6.4.

In the GENFLO model the system pressure is not constant, instead a control valve is defined for keeping the pressure in the desired range. Thus the system pressure in the first picture results in Fig. 19 only indicates, how effectively the “fictive pressure controller” works.

The first panel shows that by varying the initial coolant level by only 0.13 m the excursion power changes considerably. The results for the average and maximum fuel temperature, Fig. 19, indicate that the most important temperature jump takes place at the prompt criticality. It can be noted that the maximum cladding temperature is not in the same place as the power peaking. Thus the load into the fuel pellet cannot be seen from the maximum temperature curve. The average core temperature increases in the worst case 200 K and the maximum core temperature 250 K, but the highest enthalpy rise can be found in the location of the maximum power.

The average void fraction drops to the 0.82, when the prompt reactivity is encountered, after that in increases continuously. The core volume is 18.5 m^3. 19 % from it means 3.52 m^3. In the initial problem definition it was specified that the swell level rise 0.33 m in this variation. With the 5 m^2 of the core area this means the coolant volume of 1.65 m^3 in the core. Thus in reality no criticality could be expected with the defined boundary conditions.

The total coolant mass indicates that in the calculated variations most of the injected water remains into the reactor vessel, only a 1 % fraction is lost during a short power excursion. The strongest energy deposition takes place during the power peak, after that it is insignificant.

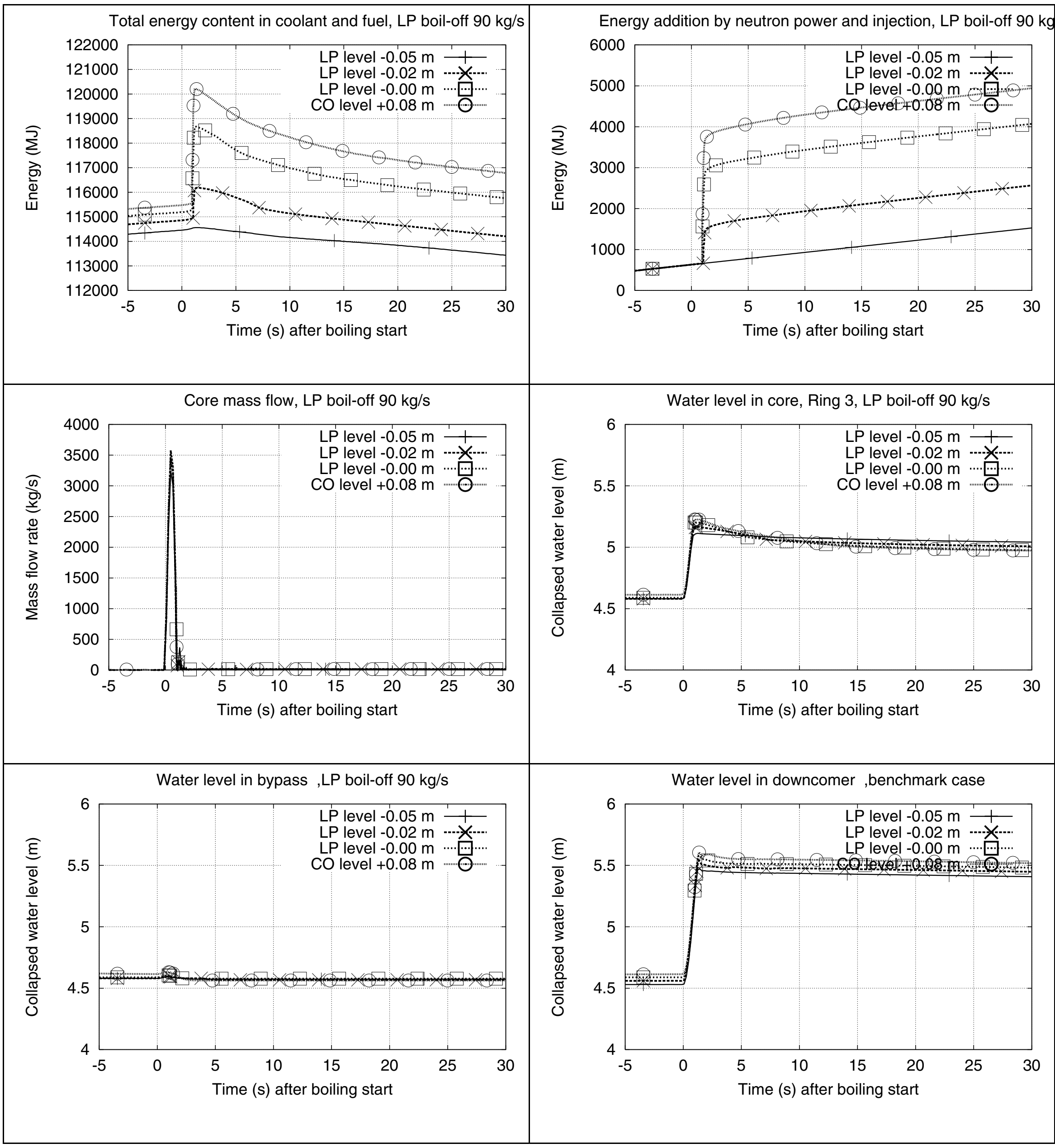

Figure 20. *GENFLO variation for the nonenergetic core flooding.*

The total energy and the core energy in Fig. 20 show, how well the energy is conserved in the integration. The energy loss of 20 % is acceptable for this type of rapid transient. The core inlet flow due to the steam injection reached maximum of 3500 kg/s as water flow, but the inlet flow decays rapidly, when the counter-current-flow situation in the lower plenum has been settled. Because the core injection includes only a short peak, no post recriticality can be achieved as in the SARA project. The water level in the core rises 0.6 m, when in the downcomer its rises nearly 1 m. The flow connection into the bypass was blocked by an assumption, that the CR melt has blocked the paths between the lower plenum and core.

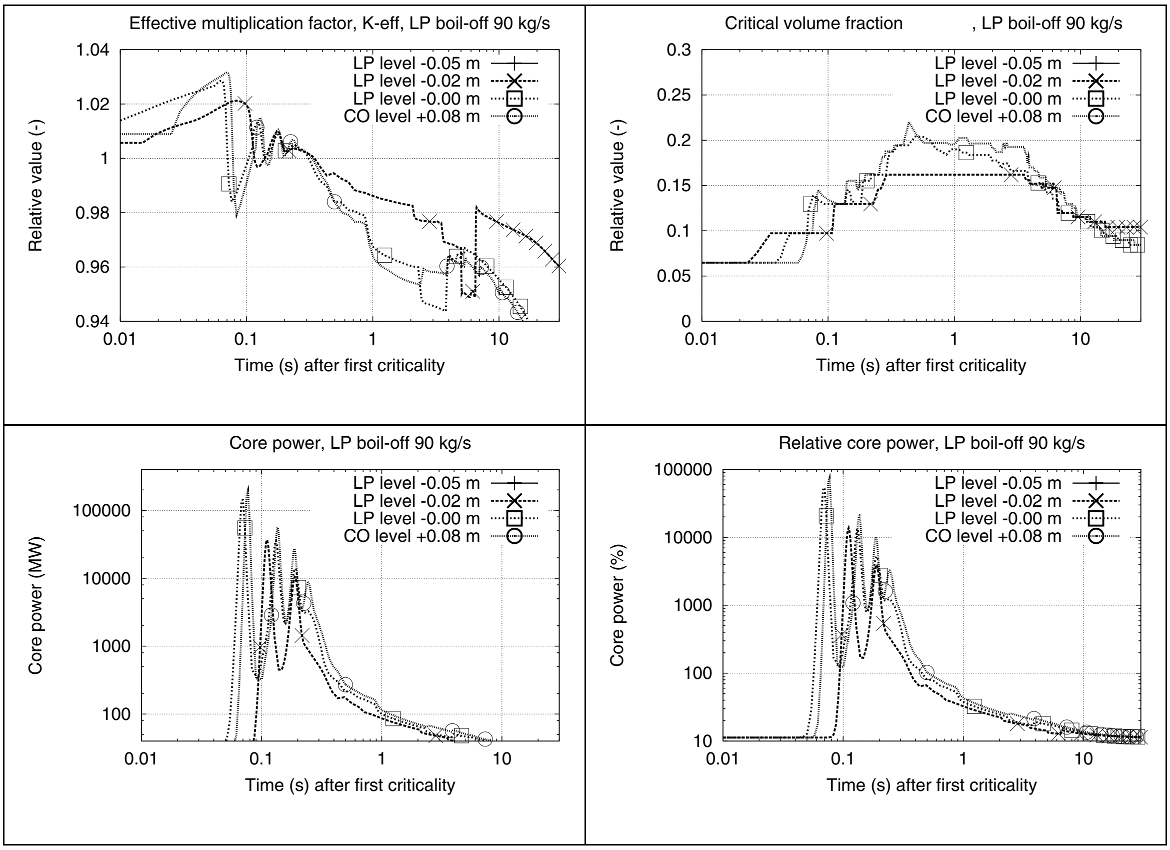

Figure 21. *GENFLO variation for the nonenergetic core flooding.*

The results in Fig. 21 show the behaviour just after the first criticality. The effective multiplication factor increases slightly in different way in different variations, thus the reactor power peaking changes on a rather large range. The fractional critical volume is around 0.13 during the first criticality, but after that still continues to rise up to the value 0.2. The maximum relative core power is 100000 MW for some milliseconds. When comparing the two results with highest power generations, saturation with the maximum power may be seen. This means that the maximum core power correlates with the level rise speed into the core and the power peak is maximum, if the level can penetrate so far that the power peak pushes it back into the lower plenum. Meantime the void fraction in the lower plenum has been established, and second recriticality peak can be expected.

The results of variations are analysed with the same procedure, as was done in the SARA project in Table 9. The relative power peak means as referred to the nominal reactor power. The result shows clearly that the prompt peak duration is really short. The maximum peak power in 65 times the nominal power. The key mechanism in stopping the power rise is the Doppler effect in the fuel.

The maximum energy deposition is calculated as (maximum power deposition into fuel) = (average power deposition) * (maximum power peaking). For the fuel integrity analysis the critical parameters is the maximum energy deposition into the pellet per unit volume. The result shows clearly that in these variations the limiting value for the energy deposition into the fresh fuel (170 cal/g), but instead the maxim deposition after the long burn-up (65 cal/g) was exceeded.

Table 9. *Comparison the results from GENFLO for the non-energetic reflooding variation. Steam flow 90 kg/s into the lower plenum.*

Variation No:	1	2	3	4
Initial level in core inlet, m	-0.05	-0.02	0.0	+0.08
Time of peak after criticality (s)	1.5	1.5	1.5	1.5
Peak amplitude, relative	no peak	10.6	55.3	65.1
Total peaking factor (-)	1	11.7	12.8	13.6
Duration of 1:st peak (s)	-	0.07	0.06	0.06
Half width of 1:st peak (s)	-	0.02	0.02	0.02
Total energy in peak (MJ)	-	1210.	2946.	3914.
Average energy addition (J/g)	-	11.78	28.6	38.1
Max. energy deposition (J/g)	-	137.8	289.8	518.2
Same as cal/g (1 cal = 4.2 J)	-	32.8	87.4	123.4
Power at end of simulation	-	0.00	0.00	0.0
Time at end of simulation (s)	-	36.	38.	38.
Max. FT at first recriticality (C)	-	1850.	1990.	2090.
Max. fuel temperature (C)	-	1850.	1990.	2090.
Max. FT at end of simulation (C)	-	1850.	1850.	1850.
Fractional critical volume at recritic.	-	0.13	0.13	0.13

Base on this analysis some uncertainty points may be listed as follows:

1. From the bypass void fraction no effect was calculated into the neutronics parameters. In this case no water level existed in the bypass zone and the analyses can be considered conservative.

2. The direct heat absorption into the coolant was defined as a prompt process. The process should be evaluated more in detail, based on the real thermohydraulic expertise.

3. In the boundary conditions defined by Sehgal and Dinh it was postulated that the water level in the core would swell 0.33 m. In the calculations 0.6 m of the water level was needed for the criticality.

4. Some studied are perhaps needed with respect to the friction parameters.

5. GENFLO nodalization did not include any division of the lower head into CRGT's and lower plenum. This feature should be included in.

6. The level swell in the lower plenum in the forest of CRGT's should be studied more exactly. The main question is, if the traditional drift flux models of narrow channels are representative enough in this geometry.

6.3. CALCULATION RESULTS FOR THE ENERGETIC FUEL-COOLANT INTERACTION

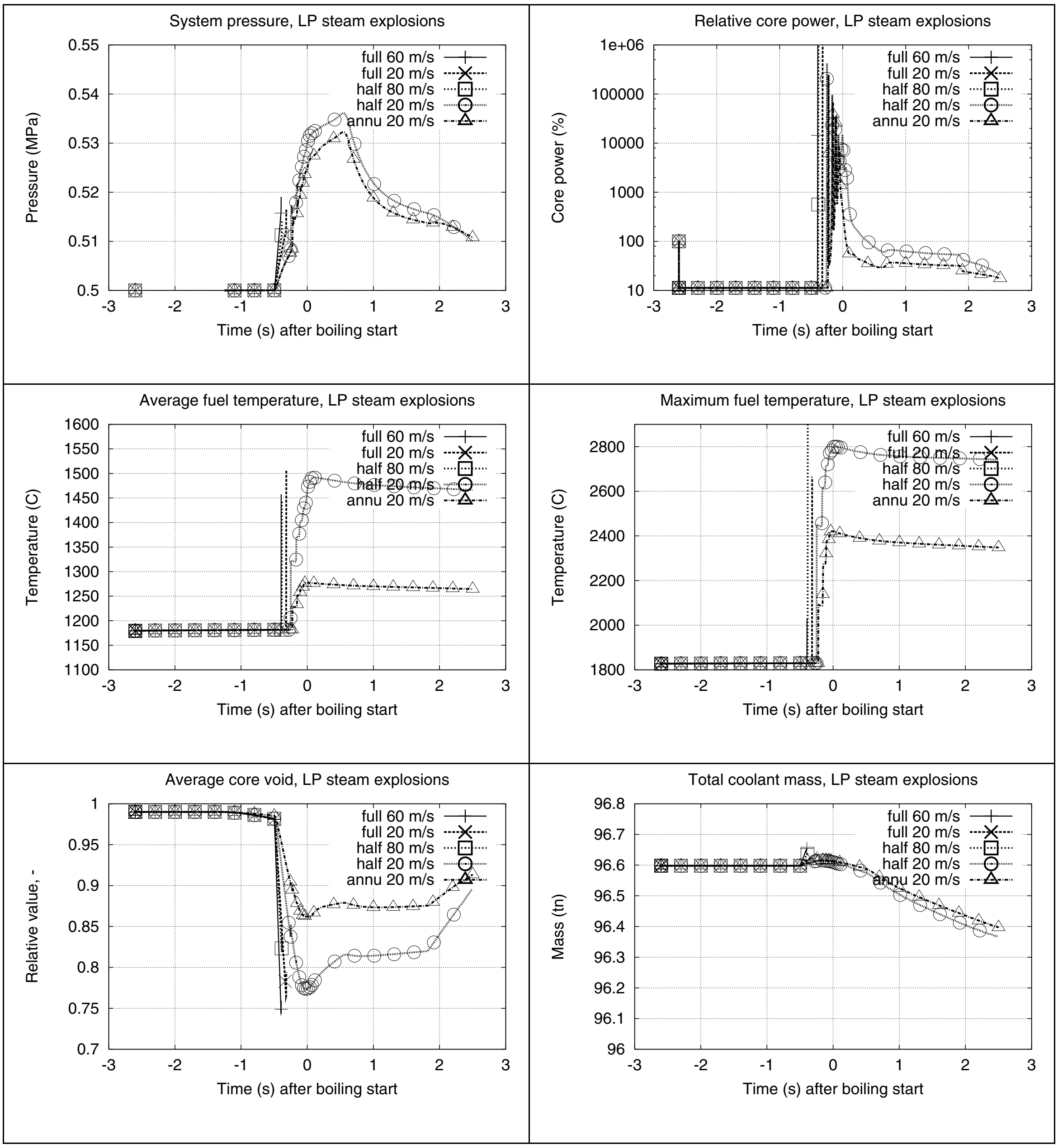

Figure 22. *GENFLO variation for the energetic core flooding.*

According to the proposal of Sehgal and Dinh (2002) four variations were calculated. In two first variations the water slug penetrates the whole core cross-sectional area, with velocity of 60 m/s during 7 ms, and with 20 m/s during 20 ms. In two other variations penetration into half of the core is assumed, with velocity of 80 m/s during 10 ms and with velocity of 20 m/s during 40 ms. As mentioned earlier, due to the 2-D cylindrical symmetry in the core model the half core geometry was calculated as a half core in the radial direction, not in the angular direction. Fifth variation was defined by selecting the half core as an annulus, i.e. no water penetration into the central core. Timing of the pulse was not explicitly modelled. The core was simulated into the recriticality, and then the marginal is calculated from the coolant volume difference compared to the proposed water movement.

The results in the Fig. 22 have a time shift. Only the two last variations were managed to be calculated into the specified end of the calculation, the half core symmetry with slow inlet velocity and annular half core with slow velocity as well. In rest of the cases the calculation stopped due to the maximum fuel temperature exceeded the pellet melting point. There was nearly no delay in this time scale between the modelled steam explosion and the recriticality.

The system pressure result indicates, how well the fictive pressure control maintained the system pressure. The interval of varying the initial levels was only 0.13 m. With this variation range the core reactivity effect changes from the negligible to the maximal achieved with the assumed water level rise into the core. The results for the average and maximum fuel temperature indicate that the most important temperature jump takes place at the prompt criticality, after that the temperatures are continuously decreasing. The rather small amount of water flowing into the core is boiled-off, and the biggest effect comes from the level jumping rapidly downwards.

The events are so quick that a void fraction at the time of recriticality is difficult to see in these results. In all cases the fuel temperatures jump significantly up.

In Fig. 23. the energy balance for two longer calculation shows that some energy is created in the rapid transient. The maximum of the plotted core inlet flow is 20000 kg/s, but if it had been possible to calculate all cases longer, the inlet flow values had been larger. The mass flow rates up to 3 seconds are valid for the half core symmetry. The water level behaves in the same way in the core and downcomer.

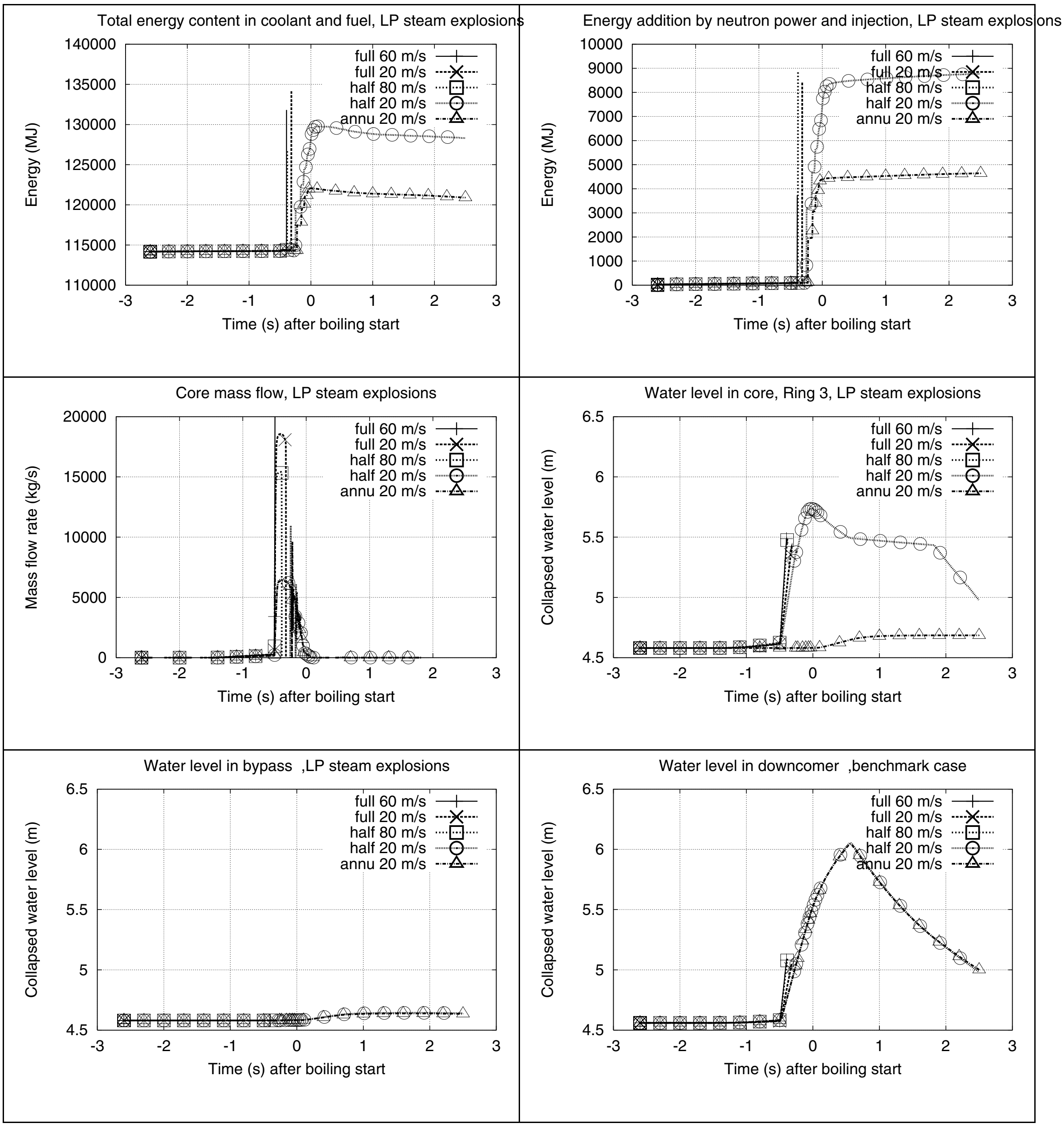

Figure 23. *GENFLO variation for the energetic core flooding.*

The results in Fig. 24 show the behaviour just after the first criticality. The effective multiplication factor increases according to the different injection velocities. The increase occurs in a slightly different way in different variations, thus the reactor power peaking changes on a rather large range. The fractional critical volume is around 0.13 during the first criticality, but in variations calculated longer after that it still continues to rise up to the value 0.2. The maximum relative core power is 1000000 MW in the variations which could not be calculated longer. Around 5-7 % of the core volume with $k_{inf} > 1.0$ has been needed for the criticality. This means 0.92 to 1.29 m^3 of the core volume. The original definition was that a 1.5 m^3 water plug penetrates the core.

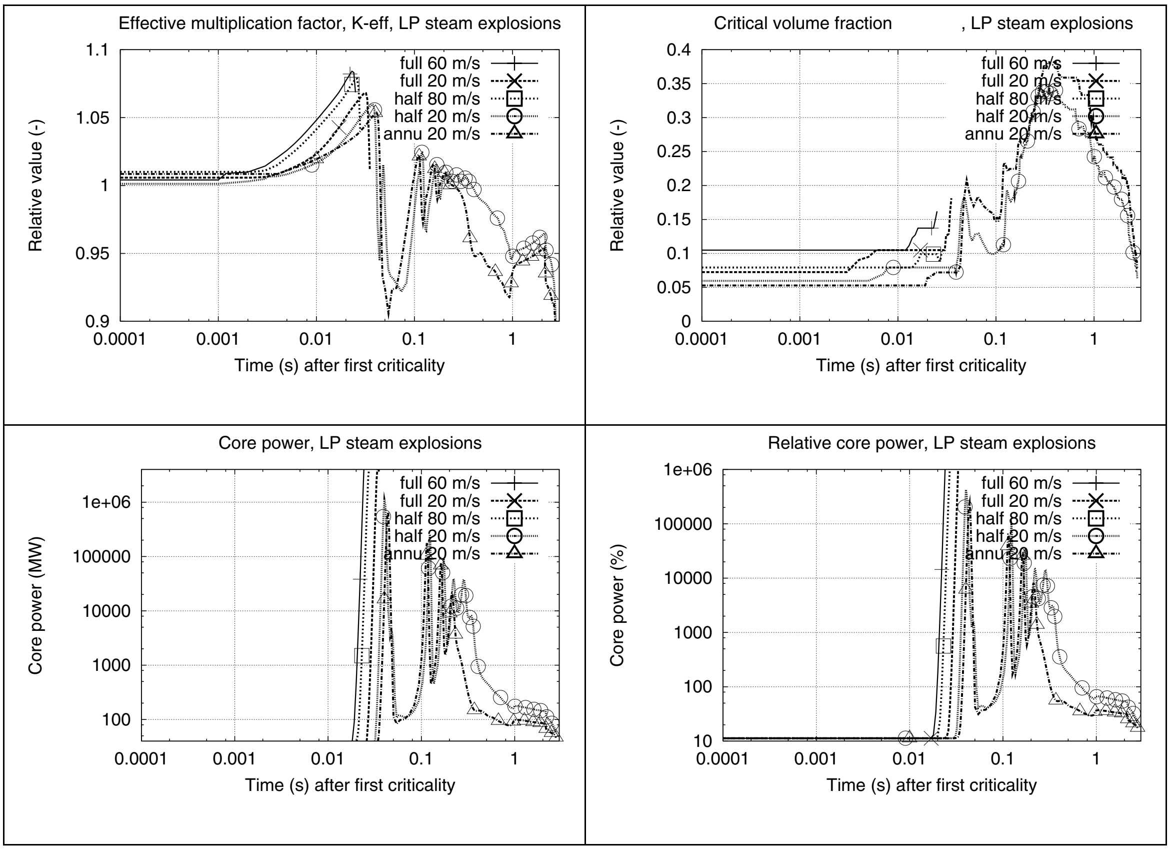

__Figure 24.__ GENFLO variation for the energetic core flooding.

__Table 10__. Comparison the results from GENFLO.

Case No:	1	2	3	4	5
Core geometry	Full	Full	Half	Half	Annular
Injection rate, m/s	60.	20.	80.	20.	20.
Time at first power peak (s)	-	-	-	-	-
Peak amplitude, relative	698.	544.	576.	396.	82.
Total peaking factor (-)	13.4	14.5	20.0	18.9	18.3
Duration of 1:st peak (s)	up	up	up	0.02	0.005
Half width of 1:st peak (s)	-	-	-	0.02	0.005
Total energy in in peak (MJ)	1391.	1517.	1368.	1523	274.
Average energy addition (J/g)	6.82	7.09	6.60	15.22	3.00
Max. energy deposition (J/g)	91.1	102.8	132.0	286.	54.8
Same as cal/g (1 cal = 4.2 J)	21.7	24.5	31.4	68.4	13.0
Power at end of simulation	max	max	max	0.20	0.20
Time at end of simulation (s)	0.1	0.1	0.1	2.5	3.5
Max. FT at first recriticality ©	2600.^	2600.^	2600.^	2850.	2400.
Max. fuel temperature (C)	2600.	2600.	2600.	2850.	2850.
Max. FT at end of simulation (C)	2600.	2600.	2600.	2750.	2350.

In Table 10 the results of variations are analysed with the same procedure, as was done in the SARA project. The relative power peak means as referred to the nominal reactor power. The result shows clearly that the prompt peak duration is really short. The maximum peak power is 698 times the nominal power. In three first cases the calculation stopped, when the fuel reached the melting temperature.

The maximum energy deposition is calculated as (maximum power deposition into fuel) = (average power deposition) * (maximum power peaking). For the fuel integrity analysis the critical parameters is the maximum energy deposition into the pellet per unit volume.

Based on this analysis some points of view may be listed as follows:

1. From the bypass void fraction no effect was calculated into the neutronics parameters. In this case no water level existed in the bypass zone and the analyses can be considered conservative. In addition to this, in the rapid transient even the time after the reactor shutdown is important for the peak effect.

2. The direct heat absorption into the coolant was defined as a prompt process. The process should be evaluated more in detail, based on the real thermohydraulic expertise.

3. In the boundary conditions defined by Sehgal and Dinh it was postulated that the water volume in the core would 1.5 m^3. The GENFLO calculations showed that core became critical with lower volumes than this value. The analyses can be considered relevant.

5. GENFLO nodalization did not include any division of the lower head into CRGT's and lower plenum. This feature should be included in.

6.4. RESULTS FROM THE NEUTRONICS SENSITIVITY STUDY

A short parameter variation was done for studying the sensitivity of neutronics related assumption. The core swell level case, where the water level is at the core entrance, was selected as the reference case. The variations were for: 1) no direct heating due to the neutronics, 2) bypass void effect considered, 3) smooth control rod profile at the melting zone.

The results in Fig. 25 show the behaviour just after the first criticality. The comparison of the results with SARA methods is done in Table 11. If no direct heating is modelled, the power increase was not limited. By taking the bypass void into the consideration, there was not a power peak. The power peak is reduced, if the core with control materials changes into a core without them on a 20 cm distance instead of an abrupt change. The short variation demostrates clearly the effect of assumption related to the neutronics area. For the more converged calculation results a new iteration with respect to the boundary conditions and neutron kinetic assumptions would be necessary.

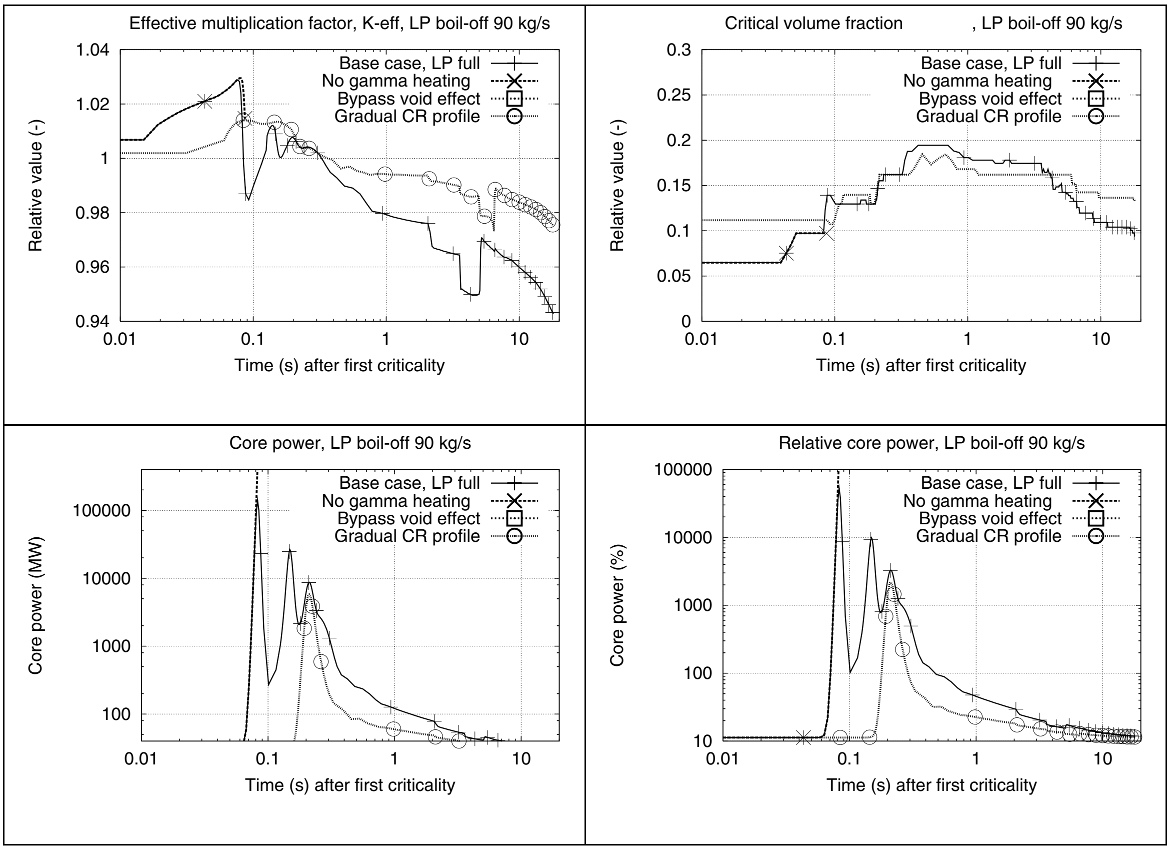

Figure 25. *GENFLO variation for the sensitivity study.*

Table 11. *Comparison the results from GENFLO.*

Case No:				
Variation	Full LP	No direct heat	Bypass void	Gradual CR prof
Peak amplitude, relative	57.9	309.	-	2.03
Total peaking factor (-)	11.7	14.3	-	9.0
Duration of 1:st peak (s)	0.01	up	-	0.02
Half breath of 1:st peak (s)	0.003	up	-	0.006
Total energy in peak (MJ)	710.	1275.	-	106.
Average energy addition (J/g)	6.0	12.4	-	1.04
Max. energy deposition (J/g)	70.2	177.3	-	9.4
Same as cal/g (1 cal = 4.2 J)	16.7	42.2		2.23
Power at end of simulation	0.	up	-	0
Time at end of simulation (s)	16.1	0.08	-	16.1

7. CONCLUSIONS

Much research has been performed in the last 20 years on energetic fuel coolant interactions. The main focus has been on in-vessel steam explosions caused by a molten corium flowing into the vessel lower head. As extreme consequence in this type of accident is the so-called α -scenario, where the conversion of the thermal energy into mechanical energy accelerates the fluid in the vessel into such a velocity that a missile is created capable of damaging the containment. The probability of this kind of large in-vessel steam explosion has recently been judged to be extremely small, however.

But the steam explosion is potentially possible also in the smaller scale, when a smaller portion of corium or metal is contacting water. During the core heat up the BWR control rods may melt first. The control rod material is accumulated on top of the core support plate and flow passages into the lower plenum are blocked. When the connections reopen the melt falls into the lower plenum water. Water is swelling due to the heat transport from melt during pouring or it is accelerated as a slug upwards after the steam explosion has been triggered.

Previous NKS and EU projects have studied BWR core recriticality, in a situation where the neutron absorbing material has been relocated and reflooding ECCS injection starts. The NKS project “Recriticality during reflooding of a degraded boiling water reactor core” and SARA project, “Severe Accident Recriticality Analysis” studied the physical phenomena as a function of the reflooding injection rate. The maximum energy deposition in fuel varied between 10 – 70 cal/g when the reflooding injection rate was around 160 – 1350 kg/s and the prompt power peaking value was consequently 0.6 to 10 times the nominal power level.

Recriticality due to steam explosion in the lower head has not been widely addressed. The analysis type requires combining together several types of simulation capabilities, 1. severe accident simulation and prediction of the control rod relocation after the core heat up, 2. evaluation of the steam generation due to the melt pouring into the lower plenum and movement of a water slug as a consequence of the steam explosion and 3) recriticality due to the level swell in the lower plenum or water slug impingement from the lower plenum into the core.

Because analysis experiences and data were available from the earlier projects, the current project was conducted as a modification of the earlier scenario. The water penetrations due to the level swell or steam explosion is similar to reflooding considered in the previous cases and also in this case the recriticality is possible. The reflooding injection rate is more uncertain in the case of the steam explosion, however. The smallest rates related to the level swell may bring the core into the critical state, but perhaps not into the prompt critical state. On the other hand the maximal velocity of the water in the lower plenum may be much higher than that of the highest reflooding rate studied in the previous projects. A multichannel estimation of the different flow routes is needed. In the third task the recriticality needs to be evaluated as a consequence water penetration into the core.

The case selected was a Olkiluoto BWR blackout calculated with MELCOR 1.8.4. Depressurisation down to the 5 bar level was assumed as the accident management feature. Relocation of control materials into lower plenum was assumed to occur at 4700 s, when all fuel is still in initial geometry and as much as possible control rod material is removed from the core area. The assumption does not maximise the steam explosion but tried to maximise the recriticality event. According to the MELCOR calculation at 4700 s water level is below core, and 13 tons of steel and 1.1 tons of B_4C are in molten state and available for relocation. At 4700 s the core maximum temperature is ~1950 K. The molten steel and B_4C have a temperature of 1700 K (MELCOR default for SS melting).

Melting of the control rod blade material produces 14.1 tons of steel making a 0.96 m level of the molten metal into the space between fuel elements. The minimum eutectic melting temperature of the relocated materials is 1150 ^oC (1423 K) and the temperature of the relocated material in between 1450 – 1700 K. This indicates that the superheat is expected to vary between 27 to 277 K in these conditions.

Two flow paths through the lower core support plate were considered: 1 through the control rod opening (=a crucifix form with a 60 cm^2 flow area) or 2 through the fuel assembly inlet (spherical form with a 78 cm^2 flow area). These result in two different assumptions for the melt pouring into the lower plenum. A control rod may be completely removed out from its location after which the control rod opening allows the melt pour down. In this case only the control rod guide tube is filled. Because the guide tube is filled with water and also surrounded by water, it is efficiently cooled. If water is swelling, it fills only the bypass. If a fuel element box wall is ablated, a flow though the fuel assembly inlet would be possible. In this case the molten metal flows into the lower plenum water and level swell both due to gradual heat removal or steam explosion could be possible.

The initial velocity of the melt flow into the lower plenum was estimated 4.53 m/s for the 1.05 m high metal pool. The initial mass flow through the 60 cm2 area is 160 kg/s and through the 78 cm2 area 209 kg/s. Based on the 200 kg/s melt flow the enthalpy flow into the lower plenum is 200 MW and the respective maximum boiling capacity 125 kg/s. All metal accumulated into the bypass area needs more than 70 seconds for the release into the lower plenum.

Without fragmentation the contact area between the molten metal and water is so small that only 0.625 kg/s steam generation in the lower plenum could be assumed. By this boiling rate no significant level swell could be achieved in the lower plenum.

If the melt stream into the lower plenum were assumed to be fragmented into 3-5 mm droplets during the fall through the lower plenum water, the steam flow equivalent through the core would be 8 m/sec. According to manual estimations the void fraction of coolant entering the core would be 30 %, the overall core reflood swell level 0.33 m and the initial water level in the core 10 cm below the core support plate. This was basis for defining the conditions for the non-energetic fuel coolant interaction case.

The recriticality analyses were done with the GENFLO computer model, which contains a 2-dimensional neutronics model allowing the calculation of the prompt criticality. The GENFLO model originates from the RECRIT code, which was used as the recriticality analysis tool previous NKS and SARA projects.

The initial assumptions were found difficult to be defined as the initial conditions of the GENFLO code, however. Instead a parameter variation was performed, where the 90 kg/s steam flow was injected into the lower plenum, giving finally the flow rate through the core as 8 m/s. The recriticality in the core was studied as a function of the initial water level in the lower plenum. The prompt recriticality conditions were achieved, when the initial water level in the lower plenum was closer than 2 cm from the core support plate. The invariant power excursion was achieved, if the initial level was at the elevation of the support plate or higher. In this case the maximum power peak is around 60 times the nominal power level. The maximum energy deposition would be around 100 cal/g, being less than the limiting value for the energy deposition into the fresh fuel, but more than the limiting energy deposition into the fuel after the long burn-up. For recriticality a higher initial water level in the lower plenum was required, than was determined in boundary conditions. Therefore the analysis results can be considered only as fictive parameter variations. They give interesting information about marginal to the possible recriticality in the case of the level swell in the lower plenum. With the proposed boundary conditions no recriticality would be encountered.

The steam explosion case presumes that after coarse fragmentation into 3-5 mm particles a triggering pressure pulse breaks the molten droplets into the less than 1 mm fraction. The pressure pulse due to the new rapid boiling is so strong that fragmentation into small fractions continues in the other part of the melt stream. If an energy conversion fraction from the thermal energy into the mechanical energy in the range of few percents is assumed, the velocity for the water slug shooting towards the core support plate can be estimated.

The first part of the study done by KTH estimated that the steam explosion condition could be bounded with two variations for the slug velocity and penetration time. In addition to the velocity variations, another variation is related to the fraction of the core affected by the water pulse. GENFLO code has a limitation that only the cylindrically symmetric core can be considered. As a combination of these postulations five cases were defined to be calculated for the energetic fuel coolant interaction. It was postulated that in the rapid penetration the slug velocity is 60 m/s and the penetration time is estimated as 7 ms. In the slow penetration the velocity of 20 m/s and the penetration time 20 ms is assumed. If only the half of the core is reflooded, the rapid penetration with 80 m/s velocity and the slow penetration with 20 m/s velocity are assumed. The rapid penetration time would be 10 ms and the slow penetration time 40 ms. In GENFLO the half core was then considered as the inner section in the cylindrical symmetry. Due to the limited possibilities in the GENFLO code, an additional variation was defined, where the outer area of the core is reflooded.

The variations were studied with the GENFLO code. The results for the rapid slug and slow slug penetration into the full core indicated that the Doppler effect can not prevent the power rise in the frame of the fuel melting limits, before 2850 ^{o}C. The water volume in the core creating the criticality was less than estimated by KTH, thus they are in agreement with KTH's postulations that the prompt recriticality can be expected in the case of the steam explosion in the lower plenum. In the two half core variations with a slow penetration the fuel temperature was maintained below the melting limit and the energy absorption was below the limiting values.

In addition to these analyses the parameter variation was done for the neutronics model. The result from this variation was that assumptions related to the neutronics part would require one iteration more for the well converged analysis result.

REFERENCES

Anttila M. 1990. Recriticality Potential in a Severe Accident at TVO plant (in Finnish) VTT YDI013/90 (1990).

Anttila, M. 1998. CASMO-4 data for Atrium fuel types 114, and 116 with 10 and 11 Ba -rods as absorbers for the lower end fuel and Atrium fuel type 115 with 9 Ba -rods as absorbers in OL-1/2 fuel, 1998-04-29.

Frid W., Hoejerup F., Lindholm I., Miettinen J., Nilsson L., Puska E. K., Sjövall H. 1999. Severe Accident Recriticality Analysis (SARA). EU INV-SARA(99)-D016, SKI Report 99:32 (Nov.1999).

Hoejerup, F. 1997a. Use of Steady-state Neutron Flux Code, TWODIM, for Dynamic Calculations, A New Approach, Working.document, INV-SARA (97)-D003, May 1997

Hoejerup F. 1997b. The RECRIT-programme and some Results from Running it, Working document, INV-SARA(97)-D006, November 1997.

Hoejerup F. et al. 1997. On Recriticality during Reflooding of a Degraded Boiling Water Reactor Core. Nordic nuclear safety research. NKS/RAK-2(97)TR-A3, February 1997.

Hämäläinen A. & Miettinen, J. 2002. GENFLO - A General Thermal Hydraulic Solution for Accident Simulation. VTT Tiedotteita - Research Notes 2163. 75 p. + app. 4 p.

Miettinen J. & Hoejerup F. 1999a. Numerical Solutions, Constitutive Correlation's and System Models of the RECRIT BWR-Recriticality Code, Technical Report, MOSES-07/99, VTT-Energy, Finland.

Miettinen J. & Hoejerup F. 1999b. Recriticality Analyses with the RECRIT Code for the Olkiluoto BWR-Plant, Technical Report, MOSES-12/99, VTT-Energy, Finland.

Miettinen J. 1999. Validation of Thermohydraulics in the RECRIT-recriticality Model for BWRs. Technical Report, MOSES-8/99, VTT-Energy.

Okkonen T.J., J. Hyvarinen, and K. Haule 1993. Safety Issues Related to Fuel-Coolant Interactions in BWRs, Proceedings of OECD/CSNI Specialist Meeting on FCI, Santa Barbara, pp. 296-308 (1993)

Sairanen R. 2001. Recriticality due to FCI in the RPV Lower Head: Initial Conditions, VTT Energy-Nuclear Energy, August 2001, ENE4-PR-6/01 (2001)

Sehgal B.R. & Dinh T.N. 2002. The Possibility and the Effects of a Steam Explosion in the BWR Lower head on Recriticality of a BWR Core, Draft NKS Report, (2002).

NOMENCLATURE

A	Flow area, m^2
Bi	Biot's number,
C_0	Drift flux distribution parameter, -
C_N	Concentration of noncendensibles in vapour, -
C_{CR}	Concentration of control rods, -
c_l, c_g	Specific heat capacity of liquid and gas, J/kg/K
c_f, c_c	Specific heat capacity of fuel and cladding, J/kg/K
D_h	Channel diameter, m
d	Droplet diamete, m
f_w	Wall friction loss
g	Constant of gravitation = 9.81 m/s^2
h_f	Wet side heat transfer coefficient (HTC) in the front, W/m^2K
h_{nb}, h_{fb}, h_{tb}	Nucleate, film and transition boiling HTC, W/m^2K
h_c	Convection HTC, W/m^2K
h_r	Radiation heat transfer coefficient, W/m^2K
h_g, h_l	Enthalpy of gas and liquid, J/kg
j_g, j_l, j_m	Superficial velocity of gas, liquid and mixture, m/s
J_g, J_l, J_m	Volumetric flow of gas, liquid and mixture, m^3/s
$K(T)$	Coefficient in Urbanic-Heidrich correlation, -
Pe	Peclet's number, -
p	Pressure, Pa
q''	Heat flux per surface area, W/m^2
q'''	Heat flux per coolant volume, W/m^3
q_g, q_l	Heat flux from wall to gas and liquid, W/m^2
q_w	Heat flux from wall, W/m^2
q_{nb}, q_{fb}, q_{tb}	Nucleate, film and transition boiling heat flux, W/m^2
Re_l	Reynolds number, -
s_g, s_l	Liquid, steam source, kg/m^3s
S_g, S_l	Liquid, steam source, kg/s
S_w	Perimeter of structure, m
Δt	Time step, s
T_s	Saturation temperature, ^oC
T_g, T_l	Gas and liquid temperature, ^oC
T_c, T_f	Cladding and fuel temperature, ^oC
T_0	Leidenfrost temperature, $T_0 = \Delta T_{Leid} + T_s$
t	Time, s
u_g, $u_{l,}$, u_m	Velocity of gas, liquid and mixture, m/s
V_{gj}	Drift flux velocity, m/s
V_{fr}	Quench front velocity, m/s
W_g, W_g, W_m	Mass flow rate of gas, liquid and mixture, kg/s
x	Steam quality, -
X_k	Pressure singular loss coefficient, -
z	Coordinate in axial direction, x

GREEK SYMBOLS

α	Void fraction
ε_w, ε_l	Emissivity of wall and liquid
λ_l, λ_g , λ_w	Thermal conductivity of water, steam and wall, W/m/K
μ_l	Dynamic viscosity of water, kg/ms
ρ_g ,ρ_l, ρ_m	Density of gas, liquid and mixture, kg/m^3
σ	Stefan-Boltzmann constant
σ	Surface tension, N/m

SUBSCRIPTS

bp	bypass
ch	fuel channel
f	friction, liquid
g	gas, vapor
gj	relative
l	liquid
L	laminar
m	mixture
T	turbulent
z	axial

ABBREVIATIONS

CRGT	Control rod guide tube
Goblin (GB)	Utility code for ASEA BWR transients, the untility and vendor expertice accumulated in the code
FCI	Fuel coolant interaction
HPCI	High pressure coolant injection
KTH	Kungliga Tekniska Högskolan
LPCI	Low pressure coolant injection

Bibliographic Data Sheet **NKS-83**

Title	Recriticality calculation with GENFLO code for the BWR core after steam explosion in the lower head
Author(s)	Jaakko Miettinen
Affiliation(s)	VTT Processes, Finland
ISBN	87-7893-140-1
Date	December 2002
Project/Sub Project	NKS/SOS-2.3
No. of pages	56
No. of tables	11
No. of illustrations	25
No. of references	13
Abstract	Recriticality of the partially degraded BWR core has been studied by assuming a severe accident phase during which the fuel rods are still intact but the control rods have experienced extensive damage. Previous NKS and EU projects have studied the same case assuming reflooding by the ECCS system. In the present study it was assumed that coolant enters the core due to melt-coolant interaction in the lower plenum. In the first case specified the relocation and fragmentation of the molten control rod metal causes the level swell in the core but no steam explosion. In the second case a steam explosion in the lower head was assumed. In the first case a prompt recriticality peak can occur, but after the peak no semistable power generation remains. In the second case the consequence of the slug entrance into the core is so violent that the fuel disintegration and melting during the first power peak may occur. After the large power peak water is rapidly pushed back from the core and no semistable power generation maintains. The fuel disintegration studies have been based on a coarse assumption that the acceptable local energy addition into the fresh fuel may be 170 cal/g, but with increasing burn-up it can be as low as 60-70 cal/g. In the level swell variations the maximum energy addition was between these limits, but in most of the steam explosion variations much above these limits. Additional variation of the assumptions related to the neutronics demonstrated that for the converged analysis result some interactions would be useful with respect to the boundary conditions and neutronic options.
Key words	Severe accidents, re-criticality, melt-coolant interaction

Available on request from the NKS Secretariat, P.O.Box 30, DK-4000 Roskilde, Denmark.
Phone (+45) 4677 4045, fax (+45) 4677 4046, e-mail nks@catscience.dk, www.nks.org.